Archaeological and Anthropological Sciences (2020) 12: 130
https://doi.org/10.1007/s12520-020-01053-x

ORIGINAL PAPER

Comparative pottery technology between the Middle Ages and Modern times (Santarém, Portugal)

Massimo Beltrame[1,2] · Fabio Sitzia[3] · Marco Liberato[4,5] · Helena Santos[2] · Felipe Themudo Barata[1] · Stefano Columbu[3] · José Mirão[2,6]

Received: 20 January 2020 / Accepted: 25 March 2020 / Published online: 9 June 2020
© Springer-Verlag GmbH Germany, part of Springer Nature 2020

Abstract

Combining historical, archaeological and experimental data, traditional and archaeological ceramics, from the Santarém district, with different chronology and functions have been studied. Our aim is to understand ancient pottery technology and to evaluate whether ceramic production followed similar principles in the Middle Ages (from the Islamic to the Christian domination) and Modern times. Moreover, traditional ceramics, knowing the productive process, have been used as a tool to interpret ancient pottery technology. We considered different utilitarian ceramic groups, namely fire, table and food-liquid container wares. Through the combination of optical microscopy (OM), X-ray powder diffraction (XRPD), X-ray fluorescence spectroscopy (XRF) with physical and mechanical tests, it has been possible to collect valuable information regarding pottery manufacturing, considering the age and the object function. Moreover, it is also considered the effect of raw materials mixing and ceramic paste preparation on ceramics final characteristics. Our results indicate that both during the Middle Ages and in Modern times, technical expertise played, and still play, a fundamental role in the creation of a specific object. In this specific case, behavioural and socio-cultural factor drove ceramists' decision when selecting between different technological solutions, and every decision or technical choice is/was taken depending on the functional and performance characteristics desired for a specific artefact. This happened during the Middle Ages, and is still happening nowadays for the production of traditional ceramics in the district of Santarém, Portugal.

Keywords Middle Ages · Modern times · Pottery technology

Electronic supplementary material The online version of this article (https://doi.org/10.1007/s12520-020-01053-x) contains supplementary material, which is available to authorized users.

✉ José Mirão
jmirao@uevora.pt

[1] CIDEHUS, UNESCO Chair of Intangible Heritage and Traditional Know-How: Linking Heritage, University of Évora, Palacío do Vimioso, Largo Marquês de Marialva, 8, 7000-809 Évora, Portugal

[2] HERCULES Laboratory, University of Évora, Palacío do Vimioso, Largo Marquês de Marialva, 8, 7000-809 Évora, Portugal

[3] Department of Chemical and Geological Sciences, University of Cagliari, Cittadella Universitaria di Monserrato (Blocco A), 09042 Monserrato, Cagliari, Italy

[4] Centre for the study of Archaeology, Arts and Cultural Heritage Sciences, University of Coimbra, Palácio de Sub-Ripas, 300-395 Coimbra, Portugal

[5] Institute for Medieval Studies, Universidade Nova de Lisboa, Avenida de Berna, 26-C, 1069-061 Lisbon, Portugal

[6] Geosciences Department, School of Sciences and Technology, Évora University, Rua Romão Ramalho 59, 7000-671 Évora, Portugal

Introduction

In every historical period pottery has always been considered an utilitarian or a symbolic-votive artefact. Its role in the construction and reproduction of social relations and cultural values is widely recognized also by social sciences (Tite and Sillar 2000). Moreover, since the Neolithic, clay-made objects always represent a conspicuous part of the archaeological findings mainly for its good resistance to weathering. This is why ceramic is one of the most studied archaeological evidence. Nowadays, various disciplines such as anthropology, archaeology and archaeometry, study this material. Also, history and ethnography, depending on the chronology, give a fundamental contribution for the understanding of ancient ceramic, especially through the analyses of historical resources and the study of rural, traditional and indigenous communities (Lindahl and Pikirayi 2010; Roux 2019; Arnold 2000). However, what can affect pottery technology and/or consequently artisans choices in the whole cycle of ceramic production? Many *variables* can influence it. Among them, we can

mention environmental restrictions, access to raw material sources (fuel, water, clay, temper) and economic or political changes.

Several authors suggest that, considering all the possible *variables*, technology can also be affected by behavioural or socio-cultural factors, such as for example ideology, religious or ethnicity. In this case, the ceramist is the major player, and every decision or technical choice is taken depending on the functional and performance characteristics desired for a specific artefact (Schiffer and Skibo 1987, 1997). The technical expertise plays also a fundamental role in the creation of a specific object and, in this case, socio-cultural factors drive potter decisions when selecting between different technological options (Sillar 2000; Lemonier 1993; Lindahl and Pikirayi 2010).

A different point of view stressed the importance of looking at the various steps of the productive cycle as being part of an interdependent system. In this case, the previous *variables* (e.g. raw materials sources) and behavioural and socio-cultural factors have the same impact on pottery technology (Tite and Sillar 2000; Gosselain 2012). In this framework, the concept of "*chaîne opératoire*", firstly coined by Lehroi-Gourhan (1964), gives a systematic description of all the steps of the productive cycle taking under consideration the whole interdependent system to understand what really influences ceramic technology. Therefore, material science disciplines such as archaeometry can give a valuable contribution for the analysis of the "*chaîne opératoire*" and to evaluate the ceramic technology. In recent years, it has also been devised the term ethno-archaeometry (Gosselain 1992). In this specific case, the different steps of the productive cycle were studied both for the analyses of contemporary pottery making communities (Cantin and Mayor 2018; Cau Ontiveros et al. 2015; Buxeda et al. 2003) and to compare contemporary ceramics with archaeological finds (D'Ercole et al. 2017; Lindahl and Pikirayi 2010). This approach has several advantages. In fact, the interpretation of traditional ceramic, knowing all the steps of the productive cycle and the technology, can help in the understanding of archaeological ceramics. Moreover, it is also possible to verify results and interpretations as well as the methodology and the assumptions used in the technological characterization of pottery (Buxeda et al. 2003).

The main focus of this work is the study of contemporary/traditional and Medieval ceramics, Islamic to Post Islamic-Christians (eleventh–sixteenth century), from the village of Muge (Municipality of Salvaterra de Magos) and the city of Santarém, district of Santarém, Portugal (Fig. 1; Table 1).

Precisely, we are going to compare the characteristics of traditional and archaeological ceramics considering different utilitarian artefacts with a specific function, such as table, fire and storage wares. Table ceramics were mainly utilized to serve and consume different type of dishes; fire ceramics were utilized to cook and consequently they were exposed to a heat source; storage ceramics were adopted to store liquid and/or food.

Traditional ceramics are still produced nowadays in Muge (Municipality of Salvaterra de Magos), in three different workshops. The owner of one of these workshops (Mr. Domingos) learned doing pottery when he was a young boy in the same village. The most ancient evidence of traditional ceramic production go back to the end of the nineteenth century (Lepierre 1899; Santos Júnior 1932). The area was already inhabited since the Iron Age, and there are evidences of pottery making since the Roman period, as evidenced by the recent archaeological excavation of the river harbour (Arruda et al. 2016). Islamic Medieval ceramics were also recovered (Lopes 2015). Archaeological medieval ceramics have been recovered inside the old city of Santarém, located at 15–20 km from Muge, during the archaeological excavation of the site "*Rua 5 de Outubro*". Also in this case, the city has been continuously inhabited since the Iron Age to Modern time (Arruda 1993; Arruda and Viegas 1999; Liberato 2016).

Our aim is to understand pottery production technology and function in the district of Santarém between the Middle Ages and Modern times. The study will be useful to understand whether or not there was continuity or change in ceramic characteristics during the Middle Ages (i.e. from the Islamic to the Christians period) and the difference, if any, with Modern ceramics. Previous studies carried out in Santarém has already discussed the continuity in raw material exploitation during the Middle Ages (Beltrame et al. 2019). Conscious of the fact that archaeological and traditional ceramics were not produced in the same workshop, we consider the analyses of Modern ceramics an interesting ethnographic approach for the understanding of ancient pottery technology. The different *variables*, behavioural and socio-cultural factors that might have affected ceramic technology in the Middle Ages will be considered in this work. To do so a multi-analytical protocol has been developed, which include petrographic (OM), mineralogical analysis (XRPD), chemical analysis (XRF), raw material sampling and analysis as well as physical-mechanical tests (i.e. density, porosity, vapour permeability, Point Load Test strength index-PLT).

In particular, the application of physical and mechanical tests to traditional and archaeological ceramics, according to methods well established in the literature (Columbu et al. 2014a, b, 2015a, b) is rarely used in archaeometry. Few authors utilized this approach in the past (De Bonis et al. 2014; Kilikoglou et al. 1998; Müller et al. 2010) mainly for the study of traditional or archaeological ceramics, but never to directly compare ceramics characteristics in the same work. The combination of physical and mechanical data to that obtained by petrography, mineralogy and chemical methods can be very useful in the understanding the production technologies related to the objects function.

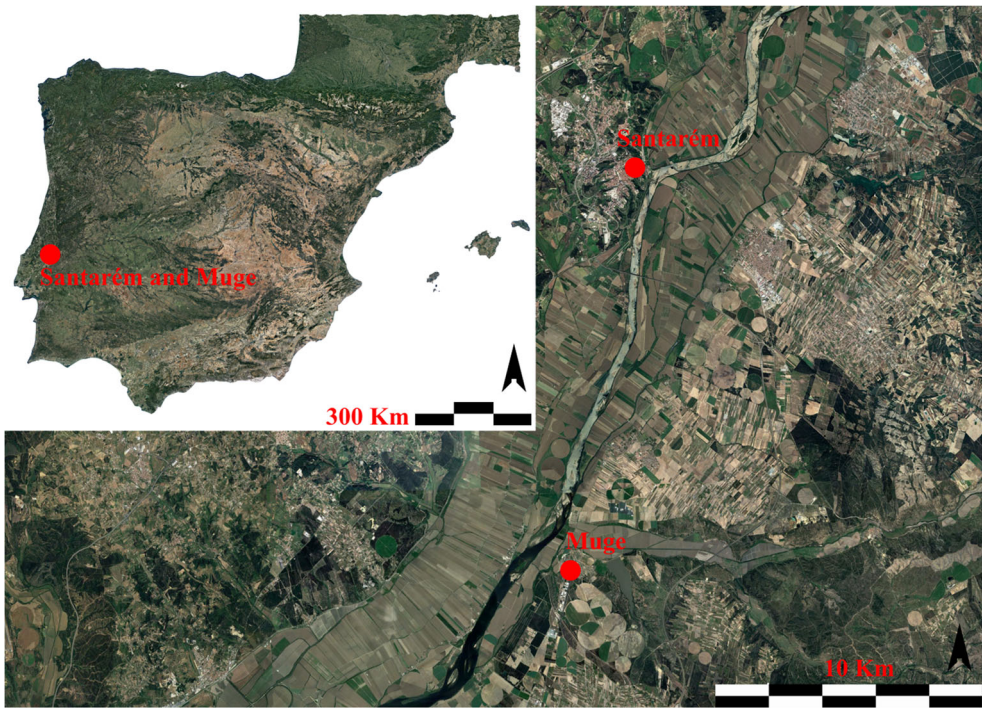

Fig. 1 Localization of Santarém and Muge in the Iberian Peninsula (top left), and the localization of Santarém and Muge in the Tagus valley. The Tagus river is located in between the city of Samtarém and the town of Muge

Geology of the area under study

From the geological point of view, the city Santarém and the small village of Muge (Fig. 1) are located in the middle of the Tagus Valley, a natural depression with orientation NNE-SSW in the southwestern region of the Iberian Peninsula, and it is part of the Lower Tagus Cenozoic Basin (LTCB).The filling of the basin happened during the Cenozoic (Cunha 2019), thanks to the combination of several factors such as the erosion proximal rocks of the basin, the evolution of the drainage system (endorheic vs. exorheic), climatic changes and different eustatic sea levels during the Miocene (Cunha et al. 2005). In the basin, three different sectors have been distinguished in the Portuguese territory: Proximal, Middle and Distal.

The Proximal sector is located in the North-eastern part of the basin between district of Castelo Branco (Beira Baixa) and Portalegre (Alto Alentejo) and in Spanish territory. It only contains continental facies. In this area, the valley is very narrow and the river excavated its path on igneous (e.g. granitoids) and metamorphic (e.g. quartzites, slates and metagreywakes) rocks of the Hercynian massif, formed during the variscan orogeny (Romão et al. 2013).

The Middle sector includes the district of Santarém (Ribatejo) and part of the Portalegre district (Alentejo), while the Distal sector includes the estuarine area of the river Tagus and the Lisbon area, close the Atlantic Ocean. These two sectors are very similar, but the Distal sector is/was more affected by the tidal sea levels. Both of them were completely covered by different Miocene and Pliocene sedimentary deposits and, afterwards, by Pleistocene fluvial terraces. Since the Later-Middle Miocene, the fluvial sedimentation is well represented and overlay the previous Palaeogene deposits. The presence of oysters on similar sedimentary record in both

Table 1 DMS geographical coordinates of Rua 5 de Outubro archaeological site (Santarém) and of Mr. Domingos' workshop (Muge). Data have been obtained using Google Earth Pro. Data degree of reliability extracted using Google Earth Pro, such as elevation and horizontal accuracy, are discussed on specialized bibliography (Goudarzi and Landry 2017; Pulighe et al. 2016; Wang et al. 2017)

Site	Geographical coordinates (DMS)					Data source
	Degree	Minutes	Seconds	Orientation	Elevation	
Rua 5 de Outubro, archaeological site	39	14	7.49	N	106	Google Earth
	8	40	45.9	W	106	
Muge, traditional ceramic workshop	39	6	17.4	N	10	
	8	42	57.06	W	10	

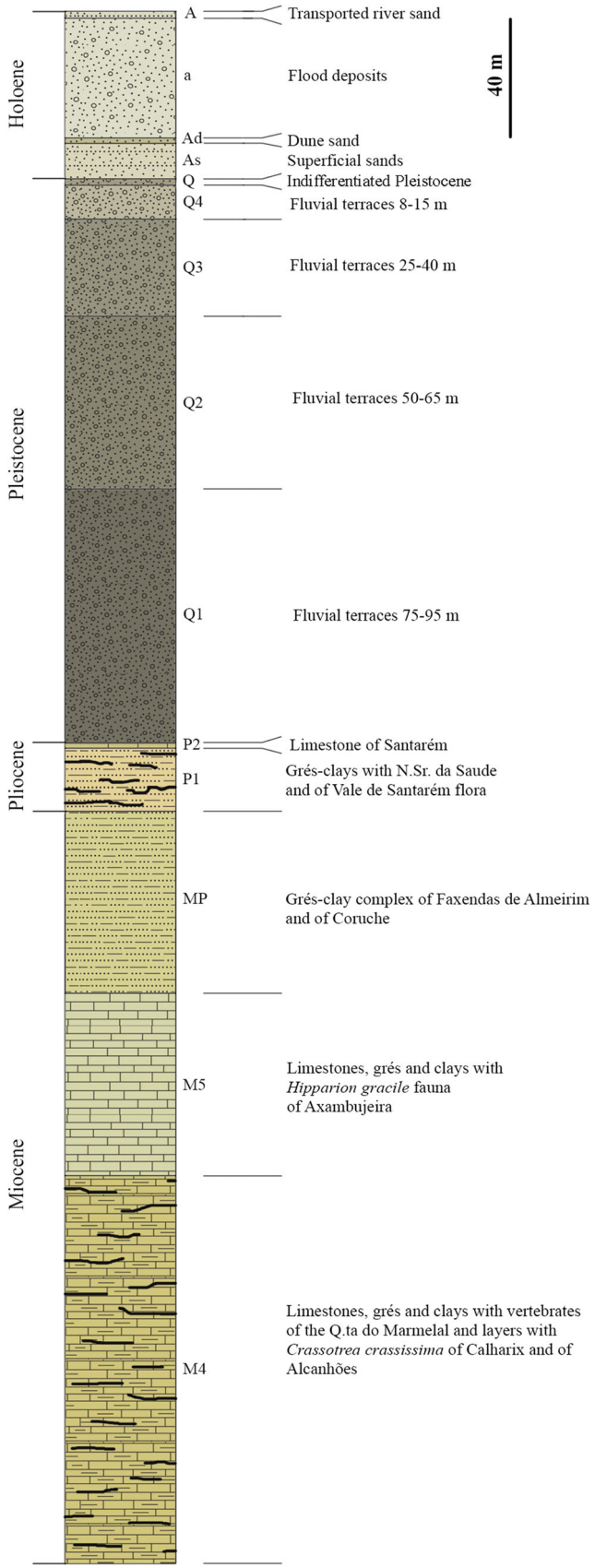

◀ **Fig. 2** Stratigraphic column of the area of Santarém and Muge. The column has been created starting from the data of the geological maps (1:50,000) of Santarém, map 31A, and of Coruche, map 31C (Zbyszewsky 1953; Zbyszewsky and Da Viega Ferreira 1968)

sectors suggests high eustatic sea levels. So, brackish water arrived at roughly 130 km far from the present coast line (Pais 2004), in the proximity of Santarém. In the upper Miocene-Pliocene, the sedimentary condition changed and lacustrine limestone are depositing.

In Figs. 2 and 3, we present the stratigraphic column and an adapted geological maps of the area of Santarém and Muge (Zbyszewsky 1953; Zbyszewsky and Da Viega Ferreira 1968). Both towns pertain to the middle sector of the Tagus basin. The town of Santarém is situated at an elevated position (at about 105 m above sea level) when compared with the river alluvial plain (which is about 9 m above sea level).

The city lay on the top of a small Pliocene plateau with a total thickness of 90 m located on the right margin of the river. The plateau can be subdivided on two different geological units (Zbyszewsky 1953). The first (*P2 layer*), with a thickness of around 3–4 m, is made of grey limestone with gastropods followed by a layer of clayey material and a layer of marly-limestone. The oldest (*P1 layer*), with a total thickness of 80–85 m, is mainly composed by interlayers of claystone and sandstone enriched in micas and/or lime concretions and with a different fossil content. The Miocene deposits outcrop at some kilometres from the city (*layers MP, M4, M5*). They represent a succession of limestone, sandstones and clay. The alluvial plain is located in front of the town (total width approximately 10 km), on the left side of the river. It is composed by modern deposits (*A, a, Ad, As*) and Pleistocene alluvial terraces (*Q, Q1, Q2, Q3, Q4*).

The area of Muge lay on the left margin of the Tagus river bank. The geology is very uniform and composed by modern flooded deposits (a), superficial sands (As) and by Pleistocene fluvial terraces (Q2–Q3), which outcrop at approximately 4–5 km from the village. In the same area, some Miocene sedimentary deposits (MP) also outcrop.

Historical context and the ceramic under study

Santarém area during the Middle Ages

Since the beginning of the Islamic domination (eighth century), the Iberian Peninsula was space of an uninterrupted opposition between two different powers/societies. The Christians, consigned in the North of the Peninsula and divided in different Kingdoms, and the Muslim in the

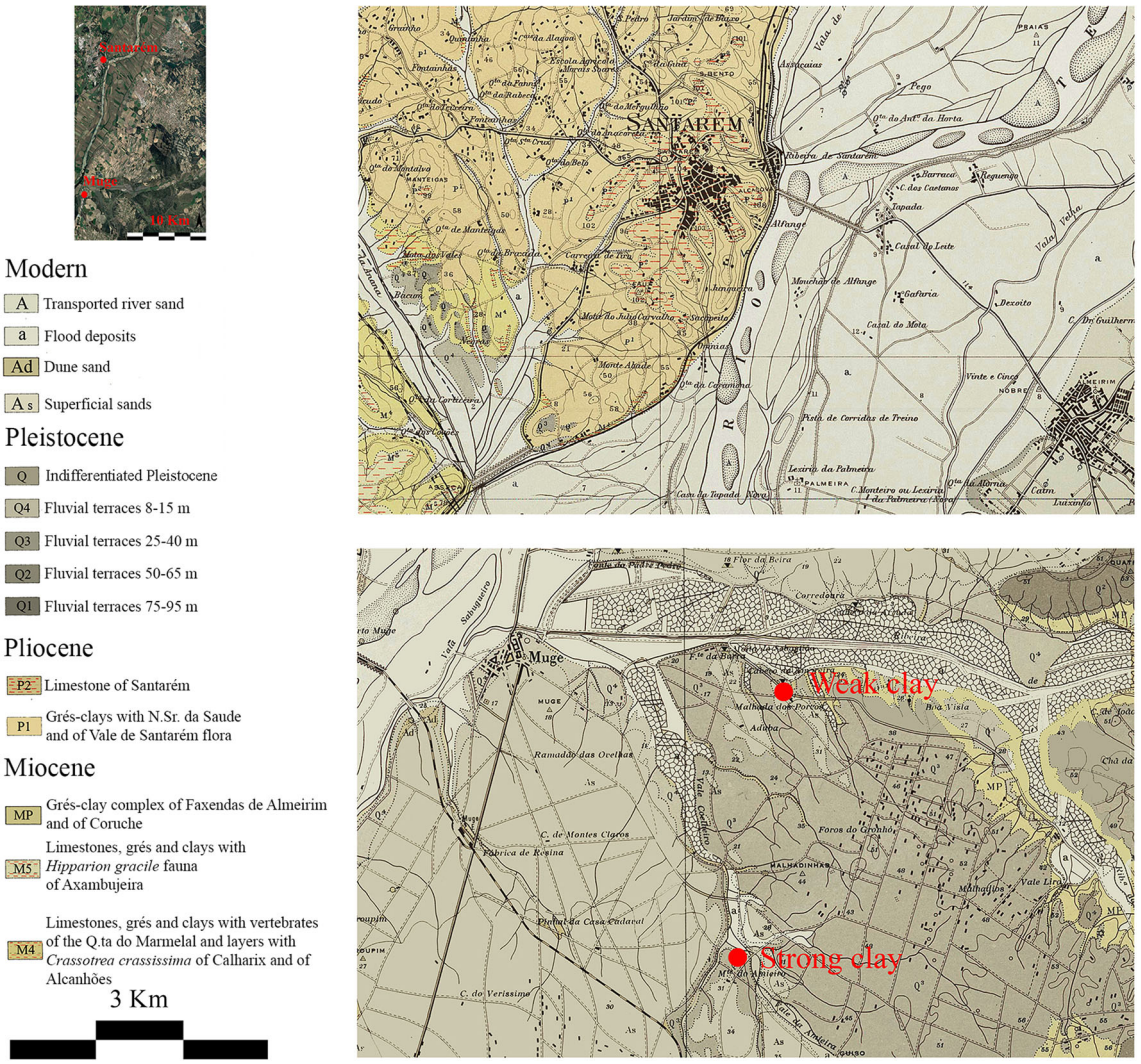

Fig. 3 Adapted from Zbyszewsky (1953) and Zbyszewsky and Da Viega Ferreira (1968), of the geological maps (1:50,000) of Santarém (map 31A, top right) and Coruche (map 31C, bottom right). The geological map also indicates where the ceramist uses to collect raw materials for the production of traditional ceramics

Centre-South, which transformed most of the *al-Andalus* (Iberian Peninsula during the Islamic domination) in a province (emirate) of the Umayyad Caliphate from Damascus. From that moment onwards, Christians kings will fight for the *Reconquista* of the ancient Visigoth kingdom of Toledo, as they considered themselves their legitimate heirs (Alves Conde 2005). Nowadays the term has a strong political and nationalist meaning, different from that of middle age (García Fitz 2009).

The city of Santarém, located in the *Garb al-Andalus* (Western Iberia during Islamic time), peacefully submitted to the Muslim at the beginning of the eighth century, maintaining several privileges such as its social, religious and economic autonomy in exchange of paying taxes to the new ruling power (Catarino 1995; Sidarus 2007). The assimilation of the Islamic culture, as well as of the new politic and economic structure by the local population, led to the creation of numerous "Mozarab" (Arabized Christians) communities (Sidarus 2007). At the beginning of the tenth century, Santarém was included in the Umayyad Caliphate of Cordova. This was a period of prosperity and stability in the *al-Andalus*. When the dynasty crumbled during the first half of the eleventh century, the political degradation led to the creation of small independent "*Taifa*" kingdoms, and Santarém was included of the *Taifa* of Badajoz (1022 AD). By the end of the eleventh century the last king of the *Taifa* of Badajoz, *Umar al-Mutawakkil*, was not able to fully control the territory. Following the continue pressure from the north and the arrival to the Iberian Peninsula of a fundamentalist Berber dynasty from Morocco, the *Almoravid*, he sought protection to *Afonso VI* of *Leão* and in exchange he delivered the cities of Santarém, Lisbon and Sintra to the Christian King of *Leão*.

The conflict between Christianity and Islam of the twelfth century assumed a different religious connotation with the arrival in the Iberian Peninsula of foreign fighters under the protection and benediction of the Roman Church to support the Iberian crusade for the *Reconquista* of Christian territories (Garcia y Garcia 2007). Nevertheless, the *Almoravids* took again the control of the Tagus valley defeating the Count *Raimundo* of Burgundy in Lisbon (1096 AD), and after a decade (1111 AD) Santarém was under the Islamic control again.

From this moment onward, the *Taifa* kingdoms disappeared and the remains of the *al-Andalus* was included in the *Almoravid* African Empire. At the beginning of the twelfth century, *Afonso Henrique* took the control of the new formed County of Portugal and he moved definitely to Coimbra. In 1139 AD he declared himself King of Portugal (Barroca 2003). With the aid of the Religious and Military order of Solomon's Temple, he was quickly able take control over the whole Tagus Valley in 1147 AD, including Lisbon and Santarém. In the subsequent years, another Berber dynasty, the *Almohad*, substituted the *Almoravid* but they were never able to restore the ancient borders of the Tagus valley and especially to takeover back.

In 1179 AD, Santarém received the "*Foral*", a royal document that regulates the politic, economic, fiscal and social set up of the city, as well as the rights of the King. In this document, it was also granted the protection to all the inhabitants, including the Islamic community. Nevertheless, during the twelfth and thirteenth centuries, the structure of the society changed radically, passing from urban, trading and tax based society during the Islamic period to a rural, feudal and stratified society (Alves Conde 2005) in the Portuguese Kingdom. Between the end of the twelfth and the sixteenth century, the city became an important river arbour opened not only to the Mediterranean, but also to the Atlantic Ocean (Liberato 2016; Casimiro et al. 2018; V. Rocha Beirante 1980). From the social point view, during the thirteenth century, the Islamic population lived freely in the city but with less rights if compared with the Christians. The historical sources attested that in the fourteenth century there were several marriages between Christians and Muslims and conversion to Christianism, suggesting a progressive assimilation of the Islamic people in the Christian society. Nevertheless since the middle of the fifteenth century, the Muslims, as well as the Jewish, were segregated in specific neighbourhood of the city (V. da Rocha Beirante 1980).

Regarding pottery, until this moment, the archaeological record of the town of Santarém did not reveal much information about its workshops and the social organization of its production. For the entire Islamic period, the only archaeological context has been excavated in Rua João Afonso (Fernandes et al. 2016), with ceramic waste and kiln rods. However, these findings assume great relevance, since they allows to attest the production of polychromatic total *Corda Seca* glaze ceramics (Beltrame et al. 2019). These data demonstrated that Santarém, during the first half of the twelfth century, was a very dynamic urban centre, synthesizing technological knowledge, in full and permanent contact with the cultural osmosis occurring in the Mediterranean area.

For the last moments of the Islamic period and the conquest of the town by the Portuguese Kingdom, four kilns were excavated during the intervention in *Rua 5 de Outubro*, nº. 2 to 8. However, only for one of them a safer chronological proposal can be advanced, due to the stratigraphic superposition with archaeological contexts with thirteenth century coins. The ceramic fragments recovered in the combustion chamber demonstrate a strong continuity with the Islamic period solutions, namely by the morphological resemblances, but mostly by the survival of the most widespread ornamental option, such as the application of white pigment motifs on the external surfaces of the ceramics.

In fact, the application of white paint until the fourteenth century (Liberato 2016) contrasts, for example, with the evolution of the ceramic record in Lisbon (Liberato 2012), where this decorative solution seems to disappear some decades after the Christian conquest of the two towns, occurred in 1147 AD. This somewhat atypical conservation of Islamic characters in the material culture of Santarém, can be complemented by historical written sources, where existence of Moorish potters is attested until the first half of the fifteenth century (V. Rocha Beirante 1980; Barros 2004).

Ceramic materials and technology

Traditional ceramics from Muge

The first work that summarized the production of ceramics in Portugal go back to the nineteenth century (Lepierre 1899). This book briefly described the regional distribution, location, the production typology (industrial or not) and the raw materials exploited for Portuguese ceramic, mentioning also the workshops of Muge. The production cycle of traditional ceramic in Muge, using the local red clay, was described by Santos Júnior (1932) and the ethnographic issues were discussed by Gomes Pinto (2012). The workshops have never changed their traditions, and the production of utilitarian ceramics is still the main activity. Nevertheless, there are less people doing this work nowadays, and the study of this activity pretend to preserve and strengthen the memory of the territory and its traditions.

Nowadays the ceramic production of Mr. Domingos in Muge is small and mainly for the local markets. The workshop is also small. We can identify four different individual spaces. In the first room, the ceramist shapes the ceramics. Afterwards there is a storing room, to store and dry ceramics. Backyard,

there is the kiln area and a big yard where the ceramist stores, treats and decants the raw clay.

Basing on the description of Mr. Domingos, the productive cycle can be summarized in three different phases: (1) extraction and preparation of the raw materials, (2) shaping and decoration and (3) firing. The ceramist uses two different raw materials: the "strong (or fat)" and the "weak (or light/slim)" clay (Fig. 4). The raw materials are extracted near the village, in a private property, with the consent of the owner. Both are located in the geological layer *Q3*, which correspond to Pleistocene fluvial terraces (Fig. 3; Table 2).

The *strong (fat) clay* is more plastic and stickier when water is added. So, we might infer that the adjective *fat* refers to the stickiness character of the clay and the adjective *strong* probably describes the ability of the wet clay to retain the stress without breaking when the artefact is shaped. On *weak (light/slim) clay*, for the ceramist, the amount of inclusions is higher. This observation will be discussed in the "Results and discussion" section with the aid of granulometric, mineralogic and chemical analysis. The two raw materials are generally empirically mixed by the ceramist, but the proportion changed depending on the artefact to be done. On fire ceramic and smaller object, the proportion of *weak clay* is higher if compared with table and food-liquid containers. So, probably, we suppose that *weak clay* expands less and it has better thermal characteristics when exposed to a heat source. Nevertheless, clay selection can be also related to other social and cultural phenomena (Livingstone Smith 2000) but, basing on the ceramist information, it looked like a technical choice. To prepare the ceramic paste, Mr. Domingos firstly decides the proportion of the two clays and he roughly powdered them manually using a hammer or a sledgehammer. Afterward, the mixture is introduced in a big tank, mixed with water and decanted for one to two days. Once most of the sand is extracted, to conclude the preparation process the finest part of the mixture is than removed from the tank and inserted into an extrusion machine to produce cylinders of homogenized pressed clay. Cylinders are than covered by a plastic thin film, in order to keep the humidity, and stored.

The ceramic artefacts are usually shaped using a vertical potter wheel moved by a simple mechanical engine. Nowadays, Mr. Domingos uses it to add temper when needed (fine industrial milled sand). The reason why the ceramist uses fine industrial milled sand is simple. He does not want to cut his finger during shaping. Shaped objects are dried in the storage room, slightly ventilated and far from the sunlight in order to allow a slow evaporation of the absorbed water. The drying time varies, depending on the season, being shorter during warmer months.

Ceramic is fired in a two chambers kiln. The firing chamber is roughly 2 × 3 m and 2 m height, and it is separated from the combustion chamber by a perforated bricks floor. Mr.

Fig. 4 Images of the *weak* (B, D) and *strong* (A,C) clay utilized in the workshop of Mr. Domingos

Table 2 DMS geographical coordinates of *weak* and *strong* clay mined by Mr. Domingos for the production of traditional ceramics. Data have been obtained using Google Earth Pro. Data degree of reliability extracted using Google Earth Pro, such as elevation and horizontal accuracy, are discussed on specialized bibliography (Goudarzi and Landry 2017; Pulighe et al. 2016; Wang et al. 2017)

Site	Geographical coordinates (DMS)					Data source
	Degree	Minutes	Seconds	Orientation	Elevation	
Weak clay	39	6	11.51	N	11	Google Earth Pro
	8	40	39.66	W	11	
Strong clay	39	4	17.45	N	24	
	8	40	56.34	W	24	

Domingos knows that the temperature inside the firing chamber is not homogeneous and that it is controlled empirically looking at the colour of the flame. He does not really know the real maximum temperature the kiln can reach. He supposes the kiln can reach more than 900 °C. The whole process of firing may take 12 h. The kiln is heated gradually to the maximum temperature. In the meantime, the entrance of the kiln is closed with bricks and then is left to cool down gradually. Usually unglazed ceramic undergoes a single firing process, while glazed ceramic are fired twice. To apply the glaze, the ceramist utilizes synthetic powdered glass product that follow the National and European regulations (National regulations: Decreto-Lei no. 190/2007).

After our visit to the workshop of Mr. Domingos, we selected 14 different utilitarian ceramics (Fig. 5; Table 3). In total, we selected 5 fire ceramics with 2 lids, 5 table ceramics and 4 liquid-food containers (liquid) with 2 lids. Most of fire and table ceramics were partially covered by glaze. Usually, just the surfaces in contact with the food or liquid were covered by glaze. On the contrary liquid-food containers were not glazed at all.

Archaeological ceramics from Santarém

Archaeological samples were recovered in the excavation of *Rua 5 de Outubro*, nº 2 to 8,in the old of Santarém. In total, we selected 27 samples (Fig. 6; Table 3) with a chronology comprised between the eleventh and the sixteenth century. Fire ceramics, table ceramics and food and liquid containers were included in the collection. With the exception of the archaeological context [520], apparently related to a metallurgical activity, all the other contexts correspond to silos filled in a short period. Therefore, they constitute very reliable samples from a chronological point of view. The archaeological contexts [520], [583], and [1667] correspond to the period between the eleventh century and the first half of the twelfth century. In fact, typical late Islamic materials were recovered. In the case of the archaeological context [476], the presence of northern ornamental solutions, such as cooking pots with punctured handles, in combination with southern pottery, appears to testify a chronology of deposition close to the integration of the city in the Portuguese kingdom, in 1147 AD. The fillings of the contexts [2466] and [2172] probably formed during the end of the twelfth century—beginning of the thirteenth century considering the recovery of first Portuguese Dinasty's coins. From the transition between the thirteenth and the fourteenth centuries, just the context [828] was studied. The materials are dominated by coarse wares with some fragments of green-glazed pottery, traditionally associated to the workshop of Paris-Rouen, France, (Liberato 2012). The chronology of the context [2059] was established thanks to the recovery of some Mudejar fragments probably from the Valencia and/or Seville regions, which appear most frequently in the territory of nowadays Portugal, from the fifteenth century onwards.

Regarding archaeological ceramics shaping method the objects could be shaped manually, in the case of artefacts with thicker walls (big earthen pots), or using the ceramist wheel (jugs, bowls, lids, pots, pans). Objects surfaces could be treated, especially bowls and pans, with the application of a slip or by surface polishing.

As already mentioned in the "Santarém area during the Middle Ages" section, the archaeological excavation in *Rua 5 de Outubro* were also identified four different kilns, which date back to the last moments of the Islamic period and just after the Reconquista of the city, twelfth–thirteenth century. During the fifteenth century, the archaeological site became a residential area and all the productive activities were probably moved to the neighbourhood of the city. The kiln typology is very similar to that excavated in Lisbon (Bugalhão and Folgado 2001) and also comparable with several other structures discovered in the Iberian peninsula during the Islamic-Post Islamic period (Coll Conesa and Porras García 2010). The kilns of Santarém (*fornos a grelha*) were circular in shape and mainly composed by two different compartments with a separated access, the fuel combustion corridor with a circular end, and the firing compartment for the ceramic, with an apse circular shape (Liberato 2012). The compartments were separated by a perforated floor supported by several pillars. From the technological point of view, previous studies (Beltrame et al. 2019) analysed some ceramic shards recovered inside the firing chamber of different kilns. Results determined that ceramics were produced locally and fired in a temperature range between 750 and 1000 °C.

Fig. 5 Traditional ceramic samples analysed in this study from Mr. Domingos's workshop

Methods

Archaeological and traditional ceramics have been analysed by optical microscopy (OM), X-ray powder diffraction (XRPD) and by X-ray fluorescence (XRF) spectroscopy. Thin sections of 30-μm thickness were prepared in an automatic polishing machine, following the "TS method" developed by Struers. To perform mineralogical and chemical analyses, a small fragment from each shard was taken (approximately 3 g). Afterwards, it was cleaned using an automatic straight grinder with a diamond tip to remove the outer contaminated layers and the glaze when present (just on traditional ceramics). The diamond tip was accurately washed with ethanol and distilled water after each sample. Subsequently, samples were washed using distilled water, dried at 40 °C for 24 h and powdered using an agate mortar. Loss of ignition (L.O.I.) was determined by calcination of dried samples (0.5 g) in a muffle furnace with a time of ignition of 1 h at 1050 °C.

Table 3 Samples list of archaeological, from *Rua 5 de Outubro* archaeological site (RCO), and traditional ceramics, from Muge (MG), analysed in this study. In the column "Arch. Context/S.U.", the numbers on square brackets report the stratigraphic unit where the archaeological materials have been recovered

[S.U.]-Ref.	Arc. Context/S.U.	Chronology—century	Typology	Function	Decoration	Arch. Site-Site
[509]-4724	[583]	11th–12th	Pot	Fire ceramics	White painted	RCO
[504]-4665	[520]	11th–12th	Pan	Fire ceramics	Unpainted	RCO
[1666]-12037	[1667]	11th–12th	Lid	Fire ceramics	White painted	RCO
[504]-4660	[520]	11th–12th	Big jug	Food, liquid containers	White painted	RCO
[504]-4666	[520]	11th–12th	Jug	Food, liquid containers	White painted	RCO
[475]-4467	[476]	11th–12th	Big earthen pot	Food, liquid containers	Unpainted	RCO
[504]-4663	[520]	11th–12th	Bowl	Table ceramics	White painted	RCO
[504]-4664	[520]	11th–12th	Bowl	Table ceramics	White painted	RCO
[91]-1978	[2466]	12th–13th	Pot	Fire ceramics	Unpainted	RCO
[2244]-15045	[2172]	12th–13th	Pan	Fire ceramics	Unpainted	RCO
[91]-1983	[2466]	12th–13th	Lid	Fire ceramics	Unpainted	RCO
[2244]-15029	[2172]	12th–13th	Big jug	Food, liquid containers	White painted	RCO
[91]-1981	[2466]	12th–13th	Jug	Food, liquid containers	Unpainted	RCO
[91]-1979	[2466]	12th–13th	Big earthen pot	Food, liquid containers	Unpainted	RCO
[91]-1985	[2466]	12th–13th	Bowl	Table ceramics	Unpainted	RCO
[829]-6952	[828]	13th–14th	Pot	Fire ceramics	Unpainted	RCO
[829]-6953	[828]	13th–14th	Pan	Fire ceramics	Unpainted	RCO
[829]-6950	[828]	13th–14th	Lid	Fire ceramics	Unpainted	RCO
[829]-6966	[828]	13th–14th	Jug	Food, liquid containers	White painted	RCO
[829]-6947	[828]	13th–14th	Bowl	Table ceramics	Unpainted	RCO
[829]-6962	[828]	13th–14th	Bowl	Table ceramics	Unpainted	RCO
[2058]-14121	[2059]	15th–16th	Pot	Fire ceramics	Unpainted	RCO
[2096]-14392	[2059]	15th–16th	Pan	Fire ceramics	Unpainted	RCO
[2058]-14124	[2059]	15th–16th	Lid	Fire ceramics	Unpainted	RCO
[2096]-14374	[2059]	15th–16th	Big earthen pot	Food, liquid containers	Unpainted	RCO
[2096]-14381	[2059]	15th–16th	Bowl	Table ceramics	Unpainted	RCO
[2058]-14122	[2059]	15th–16th	Bowl	Table ceramics	Unpainted	RCO
Trd-1	Atelier	Contemporary	Pot Lid	Fire ceramics	Unglazed	MG
Trd-2	Atelier	Contemporary	Pot	Fire ceramics	Glazed	MG
Trd-3	Atelier	Contemporary	Chestnut roaster	Fire ceramics	Unglazed	MG
Trd-4	Atelier	Contemporary	*Tacho*	Fire ceramics	Glazed	MG
Trd-5	Atelier	Contemporary	*Tacho* lid	Fire ceramics	Glazed	MG
Trd-6	Atelier	Contemporary	Jug	Food, liquid containers	Unglazed	MG
Trd-7	Atelier	Contemporary	Jug lid	Food, liquid containers	Unglazed	MG
Trd-8	Atelier	Contemporary	Water costrel	Food, liquid containers	Unglazed	MG
Trd-9	Atelier	Contemporary	Water costrel Lid	Food, liquid containers	Unglazed	MG
Trd-10	Atelier	Contemporary	Glazed plate	Table ceramics	Glazed	MG
Trd-11	Atelier	Contemporary	Painted plate	Table ceramics	Unglazed	MG
Trd-12	Atelier	Contemporary	Green bowl	Table ceramics	Glazed	MG
Trd-13	Atelier	Contemporary	Bowl	Table ceramics	Glazed	MG
Trd-14	Atelier	Contemporary	Yellow bowl	Table ceramics	Glazed	MG

Physical and mechanical properties were determined on archaeological and traditional samples (untreated samples) sized 1 × 1 × 1 cm roughly. On traditional ceramics, when glaze was present, we prepared two different samples (i.e. with and without glaze). Permeability to water vapour was also determined on some archaeological and in most traditional ceramics, with different functions, on samples sized 5 × 5 × 1 cm roughly.

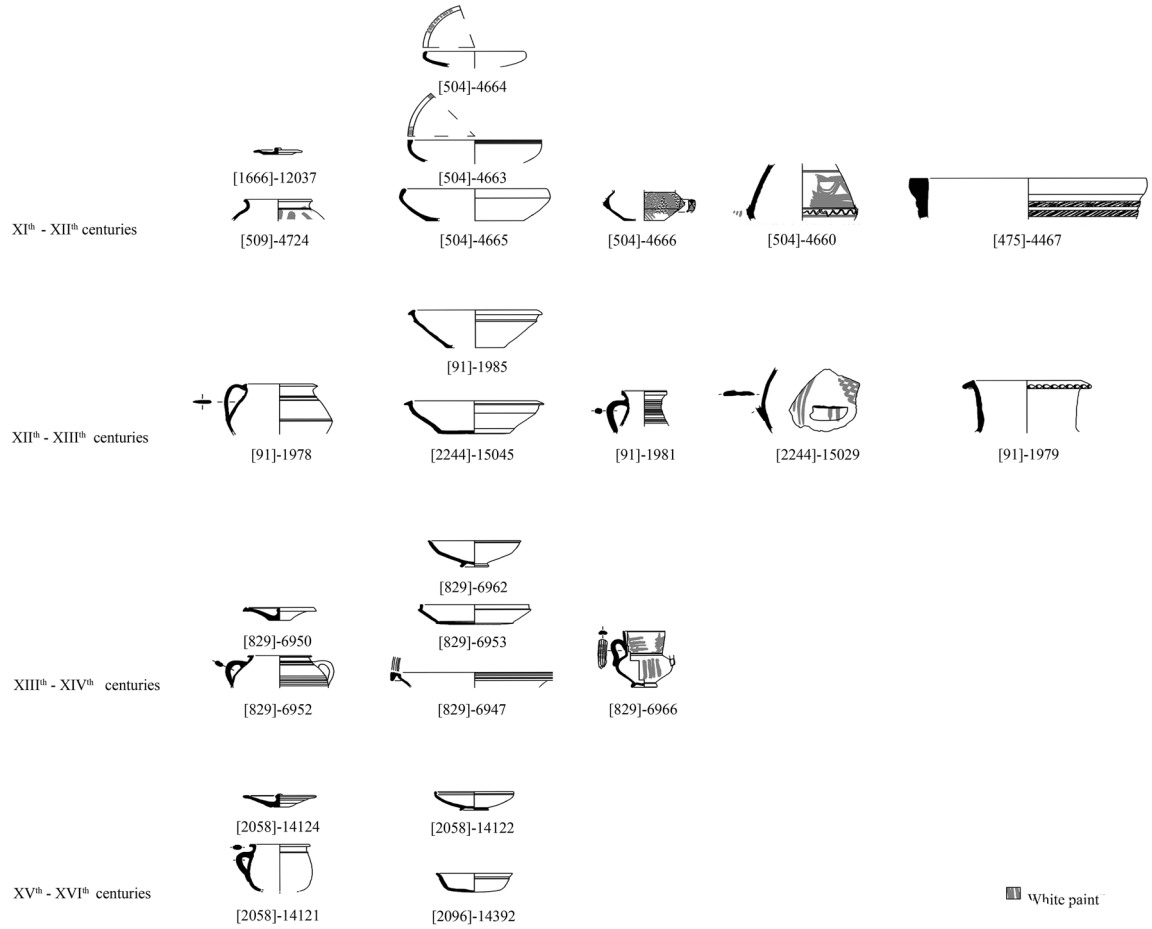

Fig. 6 Archaeological materials from *Rua 5 de Outubro* archaeological site analysed in this study

Firing experiments were performed just on traditional ceramics to evaluate the variations of mineralogical, physical and mechanical properties at different firing temperatures (750–1000 °C). This test was performed to ascertain the real firing temperature in Mr. Domingos's workshop. The experiment was conducted on different sub-samples (1 × 1 × 1 cm) with a total firing cycle of 12 h (similar to that adopted by the ceramist) using a muffle furnace under oxidized atmosphere. The muffle furnace took 2 h to reach the desired temperature, the maximum temperature was maintained for 5 h and cooling time was 5 h. Before this experiment, physical, mechanical characteristics were determined. Mineralogical (XRPD) analyses were performed in a second moment.

This study also includes the sampling as well as the granulometric, mineralogical and chemical analyses of the raw clay materials utilized by Mr. Domingos: the *strong* and the *weak* clay. Granulometric analyses were performed to evaluate sand and silt plus clay content, and the perception of the raw materials by the ceramist basing on his description. To do so, approximately 400 g of both raw materials was dry sieved using 1, 0.5, 0.25, 0.125 and 0.063 mm sieves. For grain size description, the criteria utilized for the characterization of sedimentary rocks (Adams et al. 1984) was used. Clay minerals were identified by XRPD oriented aggregates. Moreover, mineralogical analyses were performed on raw clay samples and on the < 63-μm fractions. The < 63-μm fractions were afterwards fired at 400–500–600–700–800–900–1000 °C following the same firing cycle previously described. XRPD analyses were performed just after each firing step. This experiment was developed to evaluate the mineralogical modification during firing on raw clay materials and to support experimental firing test developed on traditional ceramics described in the previous paragraph. Considering that the firing behaviour of clays is closely related with the original raw materials (clays) and the forming and firing process, chemical analyses by XRF spectroscopy were also developed, in particular on raw clay samples and on the < 63-μm fractions.

Optical microscopy applied to ceramic thin sections

Each sample was visually analysed using a transmitted light petrographic microscope Leica DM-2500P equipped with an acquisition camera Leica MC-170-HD. The mineralogy, presence of rock fragments, characteristic of the matrix, porosity, sorting and packing were described following the scheme

proposed by Quinn (2013). The degree of sphericity and grain size were described following the terminology utilized for the sedimentary rocks (Adams et al. 1984). Texture analysis, including temper percentage and modal analysis (through the estimations of the different granulometric classes) has been performed using ImageJ software 1.51k, starting from images obtained under crossed Nicols (XPL) and converted into binary images. This method have been already utilized to estimate matrix-inclusion ration on mortars (Columbu et al. 2017b) and ceramics (Beltrame et al. 2019).

X-ray powder diffraction and oriented samples

X-ray powder diffraction (XRPD) analysis was used to identify crystalline phases. A da Vinci design Bruker AXS D8 Discover diffractometer with a Cu Kα source, operating at 40 kV and 40 mA with a Lynxeye 1-dimensional detector was used. Scans were performed from 3 to 75° 2θ, with 0.05 2θ step and 1 s/step measuring time by point. XRPD were carried out on archaeological ceramics, on traditional ceramics, on subsamples of traditional ceramic fired at different temperature (i.e. 750 and 1000 °C), on *strong* and *weak* raw clay materials (oriented aggregates, raw samples, < 63-μm fractions, < 63-μm fractions fired at different temperatures). Diffract-Eva Bruker software with PDF-2 mineralogical database (The International Centre for Diffraction Data—ICDD) was utilized to interpret all XRD patterns. XRPD semi-quantitative results and reference intensity ratio (RIR) analyses (Hubbard et al. 1976) are presented for archaeological and traditional ceramics, as well as for strong and weak clay (raw and < 63-μm fractions), in different tables along the manuscript.

Bulk chemical analysis by X-ray fluorescence spectroscopy

X-ray fluorescence (XRF) spectroscopy allowed the quantification of major oxides (SiO_2, TiO_2, Al_2O_3, Na_2O, K_2O, CaO, MgO, MnO, FeO, P_2O_5). Analyses were performed operating an energy-dispersive X-ray spectrometer (EDS-XRF) S2 Puma, Bruker, using a methodology similar to that adopted by Georgiou et al. (2015). Description of the calibration method can be found elsewhere (Beltrame et al. 2019). Samples were fused on a Claisse LeNeo using a flux (Li-tetraborate) to prepare fused beads (ratio sample/flux = 1/10). The software utilized for acquisition and data processing was Spectra Elements 2.0, which reported the final oxides/elements concentration and the instrumental statistical error associated to the measurement. All results, for archaeological and traditional ceramics as well as for strong and weak clay (raw and < 63-μm fractions), are presented in a separate file annexed to the manuscript (annex 3).

Physical and mechanical properties

Physical and mechanical tests were performed on archaeological and traditional ceramic samples. Moreover, just in the case of traditional ceramic samples covered by glaze, we analysed samples with and without the glaze. The goal was to understand to which extent the glaze might influence physical and mechanical properties. The tests were also developed on different sub-samples of traditional ceramic fired at 750 and 1000 °C. Fragments with dimension of roughly 1 × 1 × 1 cm were cut, washed and dried at 105 ± 5 °C for one day prior to determine the dry masses (m_D) using an analytical balance model Sartorius R9. The real volume (V_R), on the undisturbed specimens, and the solid volume (V_S), on the powered specimens, were determined by helium pycnometer using an Ultra-pycnometer 1000 model of Quantachrome Instruments. Subsequently, the wet mass (m_W) of undisturbed specimens was determined after water absorption by immersion for 10 days. Afterwards the bulk volume V_B was calculated as:

$$V_B = [(m_W - m_{HY}) \div \rho_{TWX}] \times 100 \quad (1)$$

In formula (1), m_{HY} is the hydrostatic mass of the wet specimen and ρ_{TWX} is the water density (0.9970 g/cm^3) at 25 °C. Open porosity to water and helium ($\Phi_O H_2O$, $\Phi_O He$), closed porosity helium ($\Phi_C He$), total porosity (Φ_T), bulk density (ρ_B), real density (ρ_R) and solid density (ρ_S) were computed as:

$$\Phi_O H_2O\ (\%) = \{[(m_W - m_D) \div \rho_{TW°25C}] \div V_B\} \times 100 \quad (2)$$

$$\Phi_O He\ (\%) = \left[(V_B - V_R) \div V_B)\right] \times 100 \quad (3)$$

$$\Phi_C He\ (\%) = \left[(V_R - V_S) \div V_S)\right] \times 100 \quad (4)$$

$$\Phi_T = \Phi_C He + \Phi_O He \quad (5)$$

$$\rho_S \left(\frac{g}{cm^3}\right) = m_D \div V_S \quad (6)$$

$$\rho_R \left(\frac{g}{cm^3}\right) = m_D \div V_R \quad (7)$$

$$\rho_B \left(\frac{g}{cm^3}\right) = m_D \div V_B \quad (8)$$

Weight imbibition coefficient (IC_W) and the saturation index (SI) were computed as:

$$IC_W(\%) = [(m_W - m_D) \div m_D] \times 100 \quad (9)$$

$$SI\ (\%) = (\Phi_O H_2O \div \Phi_O He) \times 100 \quad (10)$$

Point Load strength index (Is_{50}) was determined with a Controls D550 Instrument, in accordance with the ASTM recommendations (Conshohocken 2005). The vapour permeability was determined according to Recommendations 21/85

of the Italian research council (Normal 1985) on samples sized 5 × 5 × 1 cm roughly. The technique measure the amount of vapour diffused through a circular surface area of the sample, in static condition and at regular intervals of time (24 h) until the steady state is reached. The steady state is achieved if the average value of the weight variation (ΔM), between two successive measures (considering a minimum of four values), shows an oscillation of − 5% maximum. The vapour permeability is calculated as:

$$\text{Perm} = [(\Delta M_i + \Delta M_{i-1}) \div 2] \div \pi r^2 \quad (11)$$

The first part of the equation represents the media of two values recorded on steady state, while πr^2 represent the circular surface area crossed by the vapour. The permeability to vapour is then expressed in g/m^2 × 24 h (according to ANSI-ASTM C355-64) and normalized to 20 °C. It was not possible to perform this analysis in all archaeological samples due to sampling restriction. Nevertheless, it was possible to analyse 4 tables, 2 liquid/food containers and 7 fire ceramics. On traditional ceramic we were able to perform analyses in most samples. Nowadays, permeability to vapour is usually applied in the field of conservation of cultural heritage and on the building materials (Columbu et al. 2017a; Dondi et al. 2003; Silva et al. 2009) using standardized samples. In our case, it was not possible. Traditional and archaeological ceramics had not flat and straight walls and the thickness is variable. So permeability was also normalized to the fragment thickness as:

$$\text{Perm norm.} = \text{Perm} \div d \quad (12)$$

where d is the sample thickness and the normalized value is expressed as (g/m^2 × 24 h)/mm. Considering that the firing process might influences the vitrification of the ceramic paste, and consequently its porosity (open and closed porosity), we believe that permeability to vapour can give valuable indication on ceramic technology.

Results and discussion

Optical microscope

Archaeological and traditional ceramics are similar in temper mineralogical composition and texture. The single characteristic of each samples are reported in two specific files annexed to this article (annex 1; annex 2). Inclusions are mainly composed by quartz, K-feldspar, rare plagioclase, muscovite, rare biotite, green brown tourmaline, secondary and post-depositional calcite. Among rock fragments were identified quartzite, sandstone, granitoids and, in some cases, relics of thermally altered micritic limestone. Sometimes biomicrite and intramicrite fragments were also identified (Folk 1959). Intramicrite consists of microcrystalline carbonate cement with quartz and feldspar intraclasts, while biomicrite consists of microcrystalline carbonate cement with bioclasts as foraminifera (Fig. 7F). Dispersed in the ceramic paste, in most cases, there were also unmixed clay pellets (Fig. 7G). Secondary calcite, in the form of a reaction rim, usually surrounds thermally altered or almost completely absorbed limestone fragments. In other cases, post-depositional calcite was dispersed in the ceramic paste or inside the porosity indicating contamination from the soils. The identification of thermally altered limestone fragments suggests a firing temperature, at least, comprised between 750 and 800 °C (Fig. 7C, D) or short firing time at higher temperature (Fabbri et al. 2014). Conversely, some pieces of traditional ceramic are not completely oxidized, suggesting incomplete firing (Fig. 7H). It is important to notice that secondary calcite, thermally altered micritic limestone fragments, biomicrite, intramicrite and clay pellets were never observed in traditional ceramics. These first observations suggest that the raw material was different and it was treated differently. Traditional ceramics show a more accurate homogenization of the clay.

Porosity further differentiates the two assemblages, being smaller and highly aligned to the vessel wall in the case of traditional ceramics. This is the result of the throwing shaping method adopted by Mr. Domingos, and a different pressure applied to the object during shaping.

Grain size distribution is generally unimodal in all cases. Grain shape varies from angular to sub-rounded. The most rounded and abundant fraction is mainly concentrated in the silty fraction, suggesting transport. The only exception is represented by silty sized micas crystals, generally angular and elongated. Bigger inclusions are generally sub-angular/angular in shape, indicating that temper was added to the ceramic paste depending on the object to be prepared. This is especially evident for some specific category of archaeological artefact, like liquid and food container with thicker walls (big jug-big earthen pot), such as samples [504]-4660, [475]-4467, [91]-1979 and [2096]-14374. In these cases, more temper was added if compared with jugs with thinner walls. So temper could be added depending on the thickness of the object wall in order to mitigate volume loss when the piece was dried and fired. The effect of tempering is also visible on traditional ceramics, and it was also described by Mr. Domingos. The ceramist used to add commercial milled sand to the ceramic paste. Nevertheless, if compared with archaeological ceramics, temper characteristics on traditional ceramics are uniform, and sorting is very similar between different functional classes.

OM allowed the subdivision of the shards into three different fabrics-groups (Fig. 7A–E). Fabrics 1 and 2 are from the archaeological assemblage, and fabric 3 from the traditional ceramic assemblage. In the case of fabric 3, there are no differences between objects with different function, and the

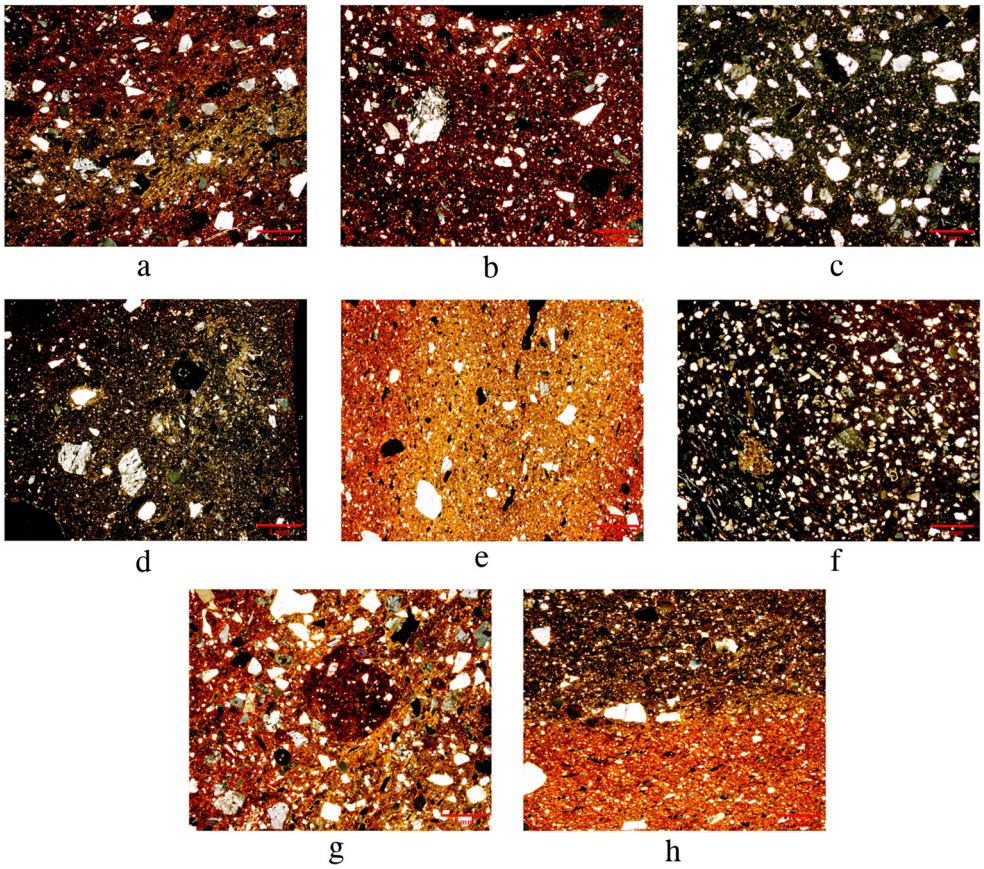

Fig. 7 Photograph collected on the OM: (A) [91]-1979 group 1/subgroup A, (B) [2058]-14121 group 1/subgroup B, (C) [504]-4660 group 2/subgroup A, (D) [829]-6952 group 2/subgroup B, (E) Trd-6 (Jug) group 3, (F) [829]-6947 group 2/subgroup A with fragment of limestone, (G) [2096]-14374 group 1/subgroup A with clay pellets, (H) Trd-3 (Chestnust roaster) group 3 incomplete firing of the peace

effect of mixing different clays adopted by the ceramist (i.e. *strong* and *weak* clays) is not visible.

Fabric 1 is characterized by an iron-rich ceramic matrix, with inclusion size up to 2.3 mm. A slip was observed in most table ceramics. The bigger inclusions were mainly observed on food-liquid containers such as big jug and on big earthen pots. The ceramic paste of fabric 2 is enriched of thermally altered or almost completely absorbed limestone fragments inclusions up to 0.9 mm. Fabric 3 has an iron-rich ceramic paste with inclusion up to 1.3 mm. Fabrics 1 and 2 present an internal variability, especially in the colour of the ceramic paste and the amount of inclusion. Sub-fabric 1A has a red ceramic paste with inclusion concentration ranging from 4.7 to 20.25%. On sub-fabric 1A are also included big food-liquid containers (big jug-big earthen pot). In sub-fabric 1B the ceramic paste is red-brown and inclusion concentration range from 8.72 to 16.87%. Regarding sub-fabrics of fabric 2, A and B, the ceramic paste is light brown\grey-brown and inclusion concentration decrease progressively from A (14.66 to 20.60%) to B (9.46%) sub-fabric. In the case of traditional ceramic samples, fabric 3, the ceramic paste is red and inclusion concentration range between 6.54 and 14.02%.

Results indicate that fabric 1 was widely utilized for the production of archaeological ceramics in all periods. In particular, sub-fabric 1A was utilized for the production of table and food-liquid container ceramics (in two cases for fire ceramics also), while sub-fabric 1B was exclusively utilized for the production of fire ceramic. Fabric 2 appears sporadically in the archaeological assemblage being utilized to create fire (2), table (1) and container (1) ceramics. Considering the characteristics observed, especially on ceramic paste and temper the raw material was probably extracted in the vicinity of the archaeological site. OM observations also reflect the heterogeneity of the sedimentary deposits of Santarém, as explained in the "Geology of the area under study" section. Clayey raw material was roughly purified and temper could be added in a second moment. Moreover, also the identification of unmixed clay pellet is another clue, suggesting that the preparation and homogenization of the clay was not that accurate.

The technology of production is very similar between the eleventh and the sixteenth centuries. Even if the kilns in the archaeological site ceased to work before the fifteenth century (the site became a residential area), the processes of making pottery (for each functional class) seems very similar on different chronological periods, indicating specialization in ceramic production (Arnold 2000). Our observations suggest that ceramics were not imported, they were all produced in the city. This suggests that the same raw material was widely available in different chronological periods without any restriction. Conversely, the production of traditional ceramics,

fabric 3, is quite similar in all cases, as evidenced by ceramic paste and temper characteristics (annex 1 and 2). There is not a clear distinction between objects with a different function (fire, table and container ceramics). At this stage, the effect of mixing different clays (*strong* and *weak* clay) adopted by Mr. Domingos is not significant. It is also not possible to appreciate specialization on traditional ceramic production because more workshops should be considered.

Comparing archaeological samples and traditional ceramics as two distinct homogeneous groups, there is a clear difference in the ceramic paste, in the inclusions characteristics, in porosity size and alignment. The ceramic paste of traditional ceramics is highly homogenous, clay pellets are almost absent, inclusions are well sorted, temper concentration is very similar between different artefacts and porosity is usually smaller and parallel to the vessel wall.

We can say that the production cycle of traditional ceramic is very similar in all cases, without significant differences between objects with different function. On the contrary, on archaeological samples it is not, and it is specialized along time. If compared with nowadays, traditional ceramics objects with different function were prepared in different way, like food-liquid containers (i.e. jugs-big jugs-big earthen pots) and fire ceramics (pots, lids, pans). All of these factors indicate a clear difference in ceramic productive cycle.

X-ray powder diffraction and raw materials granulometric analysis

In this section, X-ray powder diffraction (XRPD) is presented and discussed for archaeological and traditional ceramics (Tables 4 and 5; Fig. 8) and for raw materials (Tables 7 and 8).

XRPD of archaeological and traditional ceramics

On archaeological and traditional ceramic, quartz is confirmed as the main mineralogical phase (Tables 4 and 5). Potassium-rich feldspars and illite-muscovite are the second most abundant mineralogical phases identified, while sodium-rich plagioclases are less abundant. Haematite was identified almost in all samples. Its formation usually starts approximately at 750 °C (Maniatis et al. 1981; Nodari et al. 2007; Cultrone et al. 2004) under oxidized condition. Calcite was identified quite often on XRPD patterns, mainly in archaeological ceramics and few times on traditional ones. On archaeological ceramics, after OM, it was related to thermally altered limestone fragments with secondary calcite in the border or, in other cases, to post-depositional contamination mainly identified in the porosity system. On traditional ceramics calcite was not detected by OM. Its identification in very low amount in some XRPD patterns (Trd-3, Trd-4, Trd-6) can be associated to carbonation of some free lime after thermal decomposition of calcium carbonate present in the raw material. Calcite usually decomposes between 750 and 800 °C (Fabbri et al. 2014). Illite-muscovite peaks are always present. Usually it is supposed to disappear at a temperature higher than 950–1000 °C (Cultrone et al. 2001; Rodriguez-Navarro et al. 2003; Cultrone et al. 2004; Maritan et al. 2006). On three archaeological samples from the eleventh–twelfth and twelfth–thirteenth centuries ([504]-4660, [504]-4666, [91]-1983) mullite formed at the expense of illite-muscovite (Cultrone et al. 2004; Rodriguez-Navarro et al. 2003; Riccardi et al. 1999; Jordán et al. 1999), suggesting higher firing temperature (about 1000 °C).

The overall mineralogical composition of archaeological ceramics is quite uniform, suggesting the exploitation of same sedimentary deposit and, with some exception, most of the archaeological samples were fired in a temperature below 1000 °C (Table 4). On traditional ceramics (Table 5), in some cases, goethite and vermiculite were identified. In other cases, haematite was not identified. So, traditional ceramics were probably fired at lower temperature, maximum 750 °C, if compared with the archaeological ones. We can also extract one important methodological consideration. In both cases, XRPD patterns are not able to distinguish ceramic samples basing on its function. This result stresses the importance of OM observations in ceramic studies.

XRPD of firing experiments on traditional ceramics

The firing experiment carried out on different sub-samples of traditional ceramics (Table 5, Fig. 8) showed that illite-muscovite peaks disappeared progressively, haematite increased its intensity, and mullite, and in some cases (samples Trd-1, Trd-4 and Trd-6) portlandite appeared at 1000 °C. Portlandite forms through the reaction between the free lime and the environmental humidity (Cultrone et al. 2001) and, usually, it transforms to calcite due to carbonation. In fact, small amounts of calcite were detected on some untreated traditional ceramic samples, namely Trd-4 and Trd-6. In general, haematite is the most important mineralogical phase in order to infer the firing temperature in Mr. Domingos's workshop. In 8 cases out of 14, haematite was not identified on the untreated samples, but it was clearly identified on sub-samples fired at 750 °C. This indicates a firing temperature lower than 750 °C in many cases. So, the firing test further confirmed that the maximum firing temperature in Mr. Domingos's workshop is actually lower if compared with archaeological ceramics.

XRPD and granulometric analysis of raw clay materials

Granulometric analysis of raw clay materials The granulometric analysis of raw clay materials (*strong* and *weak* clays) evidenced that sand content is higher than silt and clay amount (Table 6). So, on both cases after the decantation process, the ceramist extracts less than the 20% of clay. Basing on the ceramist description of the raw materials, *weak* clay was supposed to be more enriched in sand content.

Table 4 Semi-quantitative XRPD results, expressed in percentage (%), of archaeological ceramics from Rua 5 de Outubro archaeological site. *Q*, quartz; *Kf*, potassium-rich feldspars; *Pla*, plagioclase feldspars; *Mus/Ill*, muscovite-illite; *Kao*, kaolinite; *Hem*, haematite; *Cal*, calcite; *Mu*, mullite; *Tr*, traces

Century	Function	Typology	[S.U.]-Ref.	Q	Kf	Na-Pla	Mus/Ill	Hem	Cal	Mu
11th–12th	Fire ceramics	Pot	[509]-4724	72	7	3	17	1		
		Pan	[504]-4665	62	17	6	15	1		
		Lid	[1666]-12037	59	18	4	18	1		
	Food, liquid containers	Big jug	[504]-4660	74	19	2		1		4
		Jug	[504]-4666	68	26	2		1		2
		Big earthen pot	[475]-4467	68	17	7	8	1		
	Table ceramics	Bowl	[504]-4663	56	15	8	20	1		
		Bowl	[504]-4664	54	22	5	18	1		
12th–13th	Fire ceramics	Pot	[91]-1978	56	9	5	30	1		
		Pan	[2244]-15045	61	17	6	15	1		
		Lid	[91]-1983	65	27	4	Tr	1		4
	Food, liquid containers	Big jug	[2244]-15029	55	21	10	13	1		
		Jug	[91]-1981	53	16	6	24	1		
		Big earthen pot	91–1979	50	26	6	16	1	1	
	Table ceramics	Bowl	[91]-1985	58	11	5	25	1		
13th–14th	Fire ceramics	Pot	[829]-6952	63	20	4	11	1	1	
		Pan	[829]-6953	59	25	3	11	1	1	
		Lid	[829]-6950	61	16	6	16	1		
	Food, liquid containers	Jug	[829]-6966	60	17	5	17	1		
	Table ceramics	Bowl	[829]-6947	44	26	15	14	1	1	
		Bowl	[829]-6962	63	20	6	10	1		
15th–16th	Fire ceramics	Pot	[2058]-14121	54	25	4	17	1		
		Pan	[2096]-14392	58	21	4	14	1	2	
		Lid	[2058]-14124	58	25	4	9	1	3	
	Food, liquid containers	Big earthen pot	[2096]-14374	50	23	7	18	1		
	Table ceramics	Bowl	[2096]-14381	69	13	4	13	1		
		Bowl	[2058]-14122	61	17	5	17	1		

Results show that the *strong* clay is actually more enriched in sand (considering the different granulometric classes) if compared with the *weak* clay (82.03% against 78.51%). Nevertheless, *weak* clay is more enriched in very coarse sand (12.64%), in very fine sand (11.51%) and in silt plus clay (20.92%). So, the enrichment in sand content described by Mr. Domingos regarding *weak* clay can be the result of two different factors. In the first case, when clays are mined, for Mr. Domingos *weak* clay might looks rougher and consequently more enriched in sand. In the second case, as evidenced by the ceramist, the raw materials were treated first in order to get rid of the bigger inclusions. Only in a second moment industrial milled sand was added. Thus, the ceramist probably referred to the enrichment of very fine sand/silt particles on treated *weak* clay if compared with *strong* clay.

XRPD analysis of raw clay materials *Strong* and *weak* clays are very similar in term of mineralogical composition. Nevertheless, some differences were observed (Table 7). On both cases, quartz, potassium-rich feldspars, sodium-rich plagioclase and rutile were identified. *Strong* clay is generally more enriched in quartz, while *weak* clay is more enriched in feldspars. If tectosilicates and oxides (i.e. rutile) are considered, on *weak* clay they represent the 65% on the raw sample and the 64% on the < 63-μm fraction while, in the case of *strong* clay they represent the 64% in the raw sample and the 57% of the < 63-μm fraction. Among clay minerals on *strong* clay, muscovite-illite, kaolinite and smectite were identified, while on *weak* clay muscovite-illite, vermiculite, kaolinite and traces of smectites were detected (Table 4). Illite-muscovite is the most represented among phyllosilicate on both raw materials, being more abundant in the *strong* clay. Smectite, vermiculite and kaolinite are less abundant. Smectite was identified by the 001 diffraction line positioned at 15.2 Å (very broad peak), while vermiculite by the 001 peak at 14.3 Å.

Table 5 Semi-quantitative XRPD results, expressed in percentage (%), of traditional ceramic samples (untreated sample, fired at 750 °C and 1000 °C). *Q*, quartz; *Kf*, potassium-rich feldspars; *Pla*, plagioclase feldspars; *Mus/Ill*, muscovite-illite; *Kao*, kaolinite; *Hem*, haematite; *Cal*, calcite; *Ver*, vermiculite; *Leu*, leucite; *Mu*, mullite; *Rut*, rutile; *Por*, portlandite; *Goe*, goethite; *Tr*, traces

Function	Sample/typology	Temp (°C)	Q	Kf	Na-Pla	Mus/Ill	Hem	Cal	Ver	Leu	Mu	Rut	Por	Goe
Fire ceramics	Trd-1/pot	Un.Sample	61	10	8	19	1					1		
		750	57	19	5	18	1							
		1000	71	22	3		1				2	1	1	
	Trd-1a/pot bottom	Un.Sample	61	10	6	22	1							
		750	56	19	5	19	1					1		
		1000	72	18	5	Tr	1				3			
	Trd-2/pot lid	Un.Sample	58	19	10	13								1
		750	55	19	8	19	Tr							
		1000	74	19	2		1				3	1		
	Trd-3/chestnut roaster	Un.Sample	53	13	10	22		1				1		
		750	51	19	6	22	1							
		1000	70	20	6	1					3			
	Trd-4/*tacho*	Un.Sample	64	14	4	15	1	1				1		
		750	60	18	5	16	1							
		1000	70	18	6	Tr	1				3	1	1	
	Trd-5/*tacho lid*	Un.Sample	63	18	5	14								
		750	63	16	4	16	1							
		1000	72	18	5		1				3	1		
Food, liquid containers	Trd-6/jug wall	Un.Sample	54	10	15	20		1						
		750	56	18	5	19	1					1		
		1000	73	17	4		1			2	3			
	Trd-6a/jug, bottom	Un.Sample	58	19	6	19								
		750	59	18	4	19	Tr							
		1000	71	18	5		1				3	1	1	
	Trd-7/jug lid	Un.Sample	62	10	7	21								
		750	56	16	6	20	1					1		
		1000	71	20	3		1			2	3			
	Trd-8/water costrel wall	Un.Sample	64	10	8	15	1					1		
		750	60	19	4	16	1							
		1000	69	22	3		1			2	3			
	Trd-8a/water costrel bottom	Un.Sample	56	19	7	17	1					1		
		750	62	17	4	17	1							
		1000	75	18	4		1				2			
	Trd-9/water costrel lid	Un.Sample	60	12	7	21								
		750	57	18	6	18	1					1		
		1000	75	17	4		1				2			
Table ceramics	Trd-10/glazed plate	Un.Sample	48	30	4	18	1							
		750	56	20	4	19	1							
		1000	73	19	4		1				3			
	Trd-11/painted plate	Un.Sample	58	10	12	21								
		750	55	19	7	17	1					1		
		1000	71	17	8		1				3			
	Trd-12/green bowl	Un.Sample	76	14	5	10	1							
		750	63	18	4	13	1					1		
		1000	70	18	6		1				3	1		
	Trd-13/bowl	Un.Sample	58	15	4	22	1		Tr					
		750	66	11	5	17	1							
		1000	71	18	4		1			2	3			
	Trd-14/yellow bowl	Un.Sample	59	14	10	16	1							
		750	59	19	4	17	1							
		1000	71	22	4	Tr	1				2			

The analysis of the oriented aggregate on *strong* clay revealed that the peak at 15.4 Å moved to 17.6 Å after solvation with ethylene glycol. This confirms the presence of smectite minerals (Moore and Reynolds 1997). In addition, when fired at 400 and 550 °C for 30 min, the smectite peak collapses close to 10 Å. In this case, we also recognized two peaks at 12.04 Å and 11.3 Å, respectively, indicating that dioctahedral vermiculite was present (Douglass 1989). In the *weak clay*, the main peak identified at 14.3 Å did not expand after solvation with ethylene glycol, but a peak appeared at 17.4 Å. So, smectite was present in small amount if compared with vermiculite. The 060 diffraction lines of both *weak* and *strong* clays further

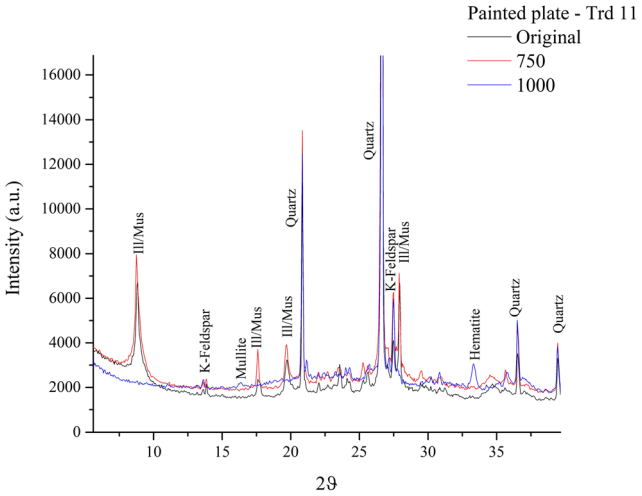

Fig. 8 XRPD diffractograms of the painted plate (Trd-11), in black untreated sample, in red the sub-sample fired at 750 °C and in blue the sub-sample fired at 1000 °C

confirmed the identification of dioctahedral vermiculite and that the smectite clay mineral is montmorillonite. In both cases, illite-muscovite and kaolinite were identified. The identification of montmorillonite explain why the strong clay is so plastic and sticky.

Firing experiments on raw clay materials

The firing experiments carried out on < 63-μm fractions of *weak* and *strong* clays were performed to evaluate mineralogical phase development during firing (Table 8). On both cases, the lack of calcium favoured mainly the formation of haematite and mullite (Noll and Heimann 2016). Calcareous raw material prevents the formation of mullite and it favours the formation of high temperature calcium-rich mineralogical phases (El Ouahabi et al. 2015; Trindade et al. 2009). Moreover, it improves the vitrification process of the ceramic past (Maniatis et al. 1981). In this case, haematite, illite-muscovite and mullite peaks can be used to understand the thermometry of the firing process. Illite-muscovite usually decomposes at 950–1050 °C, while mullite and haematite appear at 1000 °C and 750 °C respectively (Trindade et al. 2009; Rodriguez-Navarro et al. 2009; Maritan et al. 2006; Nodari et al. 2007). On our samples, montmorillonite and vermiculite 15.2 and 14.4 Å peaks disappear after the first firing cycle at 400 °C. Several authors (Kresten and Berggren 1978; McConville and Lee 2005; El Ouahabi et al. 2015) stated that montmorillonite and vermiculite might also be present at higher temperatures. In our case, after the loss of interlayer water, montmorillonite shows a diffraction line close to 9.6 Å, while vermiculite at 11.6–11.3 Å. Above 500–600 °C, it was not possible to identify anymore both vermiculite and montmorillonite, because resulted peaks were completely superimposed to illite-muscovite diffraction lines. Kaolinite disappears at 500–600 °C. Haematite was never detected at 700 °C, but it was present at 800 °C. This confirms that traditional ceramics were generally fired at lower temperature if compared with archaeological ceramics. Raw material sintering and vitrification are consistent with the complete dehydroxylation of phyllosilicates and the formation of mullite at 1000 °C. It is important to notice that neither on *weak* nor on *strong* clay calcite and portlandite has been identified if compared with untreated and fired traditional ceramic samples. In our case, fired clays were analysed just after the firing cycle and they did not have time to crystallize.

Chemical analyses by XRF spectroscopy

XRF chemical analyses of *strong* and *weak* clays (raw and < 63-μm fractions) and of ceramic samples (archaeological and traditional) are presented in separate supplementary data file annexed to this article (annex 3). Various authors make a distinction between calcareous and non-calcareous sediments/clays/ceramics based on the CaO (from limestone) plus MgO (from dolostone) content. This boundary was established between 3 wt% (Maggetti and Galletti 1982) and 6 wt% (Maniatis and Tite 1981). In our case, strong clay, weak clay and ceramics have been classified following the scheme proposed by Heimann and Maggetti (2014) and Heimann and Maggetti (2016), where the chemical concentration of SiO_2, Al_2O_3 and [CaO+MgO] is plotted in a triangular space. The triangular space is a "forecast" of the mineralogical composition that can appear during the firing process (i.e. above 950 °C) according to the chemical composition of the sample. In our case, *strong* and *weak* clays (raw and < 63-μm fractions) and all ceramic samples (archaeological and traditional) lie in the triangle comprised between quartz, Ca-plagioclase (anorthite) and mullite thus, without any distinction, the carbonate component is very low/almost absent (Fig. 9A, B). In this case, as evidenced in the "X-ray powder diffraction and raw materials granulometric analysis" section, there is no formation of high temperature calcium-rich mineralogical

Table 6 Granulometric analysis of *strong* and *weak* clays. Results expressed in percentage (%)

Sample/ granulometry	Very coarse sand	Coarse sand	Medium sand	Fine sand	Very fine sand	Silt plus clay
Strong clay	9.31	27.59	22.89	13.97	8.27	17.33
Weak clay	12.64	24.33	18.44	11.58	11.51	20.92

Table 7 Semi-quantitative XRPD results, expressed in percentage (%), of *strong* and *weak* clays: raw and < 63-μm fractions. *Q*, quartz; *Kf*, potassium-rich feldspars; *Pla*, plagioclase feldspars; *Mus/Ill*, muscovite-illite; *Kao*, kaolinite; *Rut*, rutile; *Smc*, smectite; *Ver*, vermiculite; *Tr*, traces

Function	Typology	Fraction	Q	Kf	Pla	Mus/Ill	Kao	Rut	Smc	Ver
Raw clay materials	*Strong* clay	Raw	37	24	2	28	2	1	6	
		< 63 μm	36	16	4	33	4	1	6	
	Weak clay	Raw	27	29	8	25	3	1	Tr	7
		< 63 μm	31	25	7	27	3	1	Tr	5

phases. The concentration of Al_2O_3 and of SiO_2 is very similar for all samples. The first ranges between 16.6 and 22.9 wt%, and the second between 65.20 and 73.20 wt%. Nevertheless, some differences were evident. Generally, on archaeological samples CaO concentration is between 0.51 and 3.57 wt%, while traditional ceramics do not contain more than 0.5 wt% of CaO. The MgO/Fe_2O_3 ratio is generally lower on archaeological ceramics ($MgO/Fe_2O_3 < 0.2$), with the exception of sample [829]-6947 ($MgO/Fe_2O_3 = 0.31$). The absolute concentration of MgO and Na_2O (Fig. 9C) is higher on traditional ceramics. Nevertheless, some archaeological ceramics, from the 13th–14th and 15th–16th century, are slightly enriched in Na_2O ([829]-6952, [829]-6962, [2058]-14124) and they partly overlap the traditional ceramic group. Three of them, excluding the sample [829]-6962, are included on fabric 2 and they pertain to fire and table ceramics. Differently from XRPD, in this case, XRF results are able to differentiate different fabrics but not ceramics with different function. In any case, the results collected for archaeological ceramics, point to the exploitation of the same raw material as suggested by XRPD and OM results, and small difference in chemical composition can be the result of the heterogeneity of the sedimentary deposits of the town of Santarém as explained in the "Geology of the area under study" section. Chemical analyses, even if small differences are evident between traditional and archaeological ceramics, show that the overall chemical composition is very similar. Actually, raw materials were extracted in different places but they pertain to the same sedimentary basin. So, this result further support XRPD results and the identification of similar mineralogical phases in archaeological and traditional (i.e. untreated samples, fired at 750 and 1000 °C) is justified.

Table 8 Semi-quantitative XRPD results, expressed in percentage (%), of the mineralogical phase evolution during firing of *strong and weak* clays (with grain size < 63-μm fraction). *Q*, quartz; *Kf*, potassium-rich feldspars; *Pla*, plagioclase feldspars; *Mus/Ill*, muscovite-illite; *Kao*, kaolinite; *Rut*, rutile; *Smc*, smectite; *Ver*, vermiculite; *Hem*, haematite; *Mul*, mullite; *Tr*, traces

	Typology	Fraction	Firing T.	Q	Kf	Pla	Mus/Ill	Kao	Rut	Smc	Ver	Hem	Mul
Raw clay materials	*Strong* clay	< 63 μm	0	32	17	4	33	7	1	6			
			400	35	18	4	37	6	1	Tr			
			500	41	15	4	39	Tr	1	Tr			
			600	42	17	4	37		1				
			700	43	17	3	36		1				
			800	39	17	5	38		1			1	
			900	55	17	5	21		1			1	
			1000	74	17	2	Tr		1			2	3
	Weak clay		0	32	22	6	28	5	2	Tr	5		
			400	35	20	6	32	6	2		Tr		
			500	38	17	8	36	Tr	1		Tr		
			600	42	16	6	35		1		Tr		
			700	43	11	6	37		2		?		
			800	38	17	11	32		2			1	
			900	60	17	5	15		1			1	
			1000	77	14	2			1			2	2

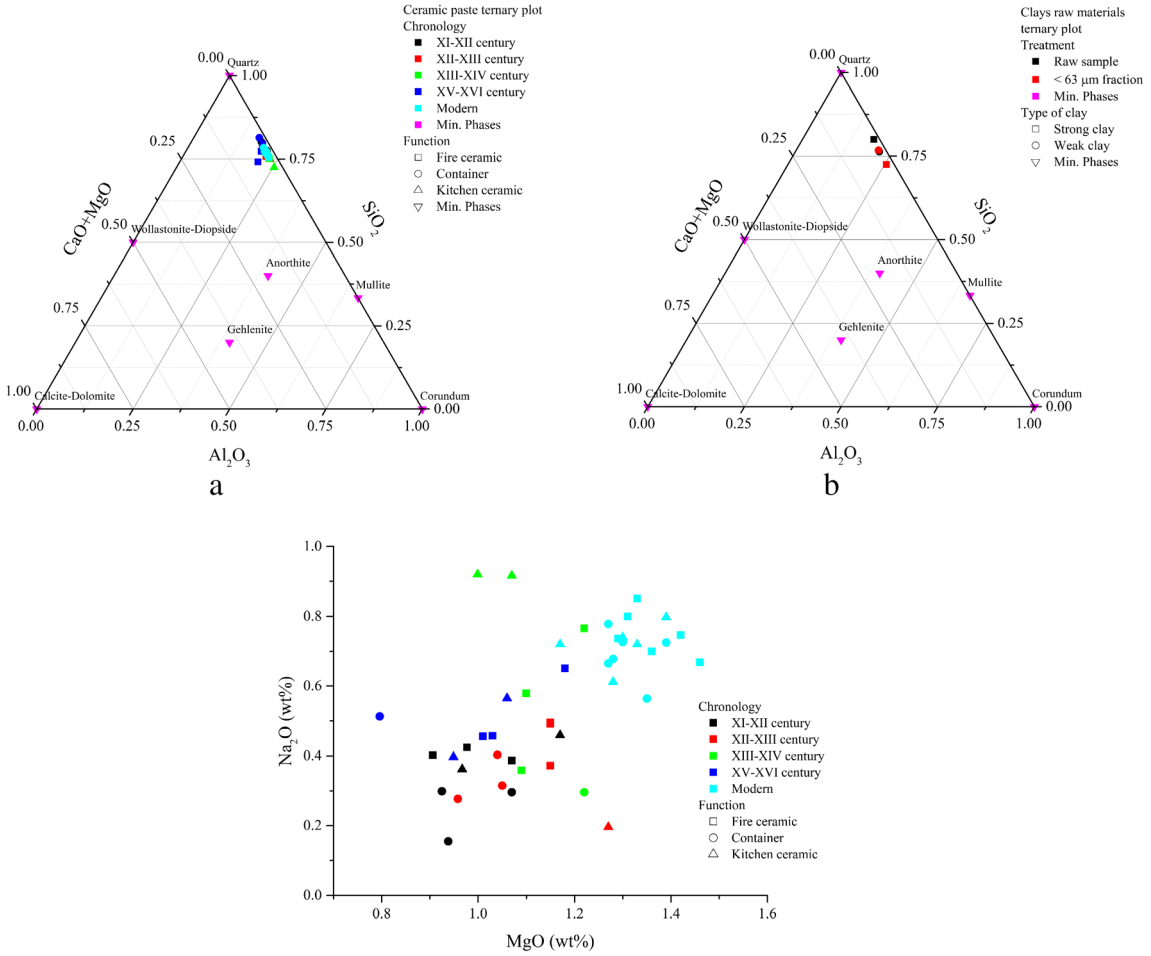

Fig. 9 (A, B) SiO_2, Al_2O_3, [CaO+MgO] ternary diagram of the strong and weak clay (raw and < 63-μm fractions) and of the ceramic samples (i.e. archaeological and traditional) after Heimann and Maggetti (2014, 2016). (C) Binary graph of MgO and Na_2O of archaeological and traditional ceramic samples

In the case of *strong* and *weak* clay (raw and < 63-μm fractions), they generally follow the same pattern identified for traditional ceramics. The main differences reside in the SiO_2 and Al_2O_3 content. In the strong clay, SiO_2 concentration drops from 65.9 to 56.6 wt% and, at the same time, Al_2O_3 concentration increase from 15.2 to 19.9 wt% in the < 63-μm fraction. At the same time, also MgO, Fe_2O_3 and K_2O concentration increase. These results point to a strong increase in clay content in the finer fraction of the sediment. On the contrary, on *weak* clay SiO_2 concentration increases from 60.5 to 61.6 wt% while Al_2O_3 remain quite stable, being 17.2 in the raw sample and 17.1 wt% in the < 63-μm fraction. Thus, the ratio between sand and clay seems to remain the same. These results further support granulometric and XRPD analysis carried out on *strong* and *weak* clays suggesting that, in the finer fraction, the content of silty sized grains is higher on the *weak* clay.

Physical and mechanical properties and correlation with compositional features

Physical (i.e. density, porosity, permeability) and mechanical (i.e. punching strength index) ceramic characteristics are quite heterogeneous, especially between different functional classes. Considering ceramic samples like two different homogeneous groups (i.e. archaeological and modern), total porosity (Φ_T) made the first difference. The mean values (Table 9, Fig. 10A) of all functional classes from different periods showed that traditional ceramics are more porous than archaeological ceramics. Normally ceramic porosity can be influenced by temper amount and size, by firing temperature and also by the pressure made by the potter when modelling the pot and kneading the paste. One would expect higher porosity on ceramic with bigger inclusion and more temper (archaeological ceramics), because of structural discontinuities between temper grains and the ceramic paste (Allegretta et al.

Table 9 Mean values for physical and mechanical properties of archaeological ceramics (from the eleventh–sixteenth century range), traditional-modern ceramics (untreated samples) and traditional-modern ceramic sub-samples fired at 750 °C and 1000 °C

Century		Apparent density g/cm^3 ρ_B	Real density g/cm^3 ρ_R	Solid density g/cm^3 ρ_S	Total porosity % Φ_T	Open porosity to water % $\Phi_O H_2O$	Open porosity to helium % ΦOHe	Closed porosity to helium % ΦcHe	Weight imbibition coefficient % ICw	Saturation index % SI	PLT strength index (MPa) $Is_{(50)}$
11th–12th	Average	1.93	2.61	2.72	30.0	22.8	26.0	4.0	11.9	87.6	2.47
	St.dev.	0.05	0.05	0.09	2.8	2.9	2.5	3.0	1.9	7.1	0.78
12th–13th	Average	1.91	2.61	2.71	30.4	24.0	26.8	3.6	12.6	89.7	4.07
	St.dev.	0.04	0.04	0.06	3.4	1.8	2.2	2.3	1.2	5.4	1.42
13th–14th	Average	1.91	2.59	2.72	31.0	22.5	26.1	4.9	11.8	86.9	3.57
	St.dev.	0.04	0.11	0.05	2.3	3.1	3.9	3.0	1.8	5.5	1.25
15th–16th	Average	1.93	2.64	2.69	29.0	24.4	27.0	2.0	12.8	90.3	2.71
	St.dev.	0.06	0.05	0.03	2.4	2.9	2.6	1.3	1.6	5.9	0.93
Modern, untreated	Average	1.85	2.64	2.73	33.3	26.9	29.9	3.4	14.5	90.1	2.48
	St.dev.	0.02	0.06	0.06	1.9	1.1	1.4	1.8	0.6	5.0	0.76
Modern 750 °C	Average	1.87	2.68	2.76	32.9	26.1	29.9	3.0	13.9	87.6	2.66
	St.dev.	0.04	0.07	0.07	2.6	1.3	2.3	1.8	0.8	6.3	1.01
Modern, 1000 °C	Average	1.94	2.61	2.74	30.3	21.3	25.7	4.7	11.0	83.5	3.95
	St.dev.	0.03	0.05	0.08	2.4	1.1	1.5	2.3	0.7	6.4	2.25

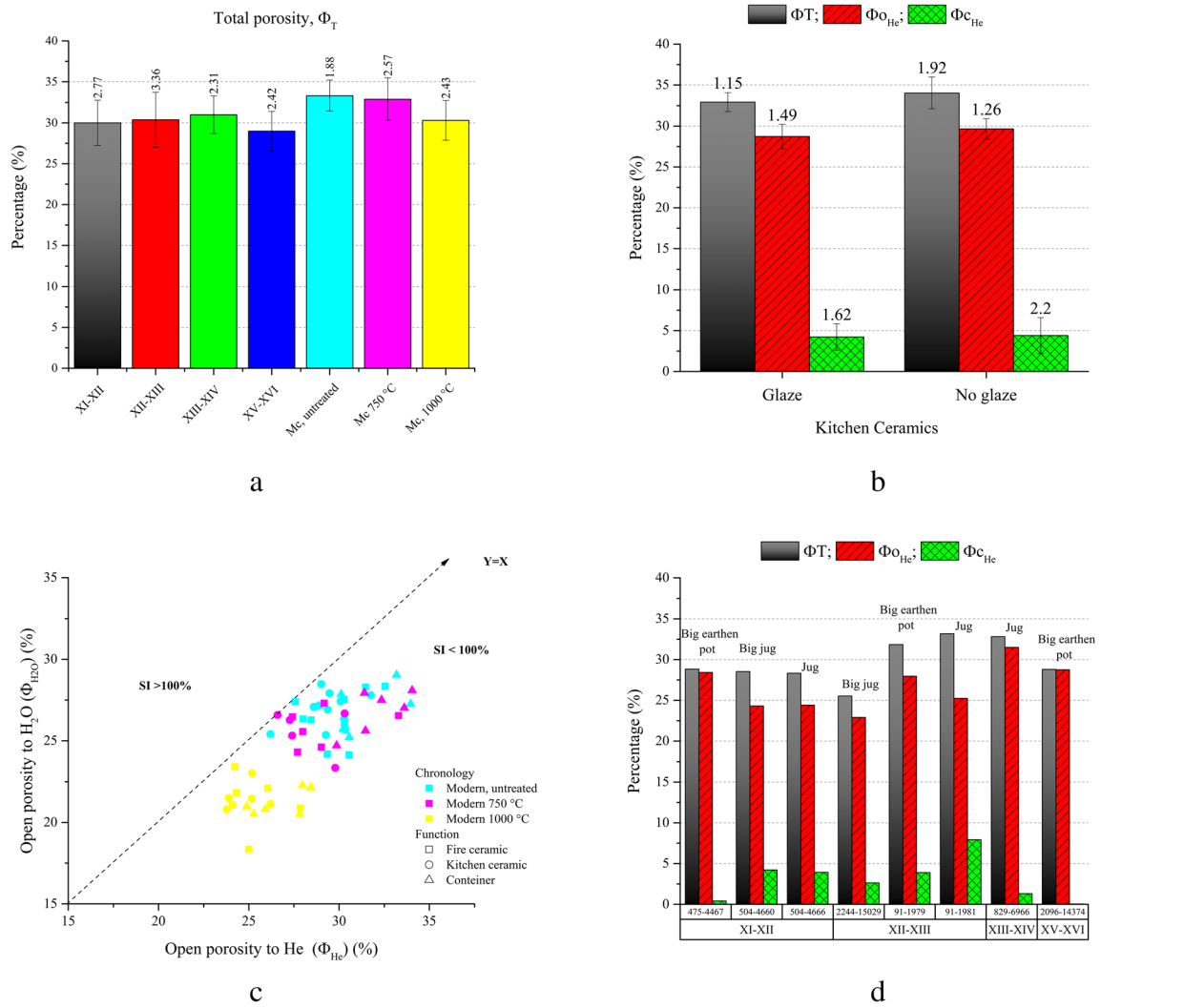

Fig. 10 Physical properties of archaeological and traditional ceramic samples: (A) Φ_T medium values with standard deviation of archaeological, traditional and firing experiment on traditional ceramic samples; (B) Φ_T, Φ_OHe and Φ_CHe medium values of traditional table ceramic samples with glaze and without glaze; (C) Φ_OHe, $\Phi_O H_2O$ and S.I. values of raw traditional ceramic samples, fired at 750 °C and fired at 1000 °C; (D) Φ_T, Φ_OHe and Φ_CHe of archaeological food-liquid container ceramic samples

2014; De Bonis et al. 2014; Müller et al. 2010). In any case, after OM observation, a clear difference in porosity size and alignment was evident, but it was not possible to establish the exact amount on traditional and archaeological ceramics. The effect of the firing temperature is widely discussed in the bibliography, and when firing temperature increase porosity decreases consistently due to the vitrification of the ceramic paste (Kam et al. 2009; De Bonis et al. 2014). In particular, ceramics with similar mineralogical and chemical composition should follow the same transformation during firing. In this case, considering XRPD results, physical and mechanical characteristics suggest that ancient Middle Ages kilns in Santarém worked at higher temperature if compared with Mr. Domingos's kiln. Nevertheless, even if traditional and archaeological ceramics were fired at different temperature, in both cases, specific criteria were adopted for the production of fire, food-liquid container and table ceramics. All singular sample value, medium values for functional class and chronological period of physical and mechanical properties can be found in a specific file annexed to this article (annex 4).

Traditional ceramics

The results obtained by OM, XRD and XRF analyses showed that traditional ceramics apparently represent a homogeneous group. The difference between different functional classes (fire ceramics, food/liquid containers, and table ceramics) resided in the clay mixture prepared by the ceramist (i.e. *strong/weak* clays ratio) and it is not appreciable by OM, XRPD and XRF analyses. Instead, the comparison of ceramics' physical and mechanical property results shows specific characteristics depending on the sample. Considering the mean values for each functional class (Table 10) the results show that (i) table ceramics have an intermediate value of total porosity (Φ_T),

Table 10 Mean values with standard deviation for physical and mechanical properties of untreated modern ceramic samples (without glaze when present), and traditional-modern ceramic sub-samples fired at 750 °C and 1000 °C from different functional classes

Function	Firing temperature		Apparent density g/cm^3 ρB	Real density g/cm^3 ρR	Solid density g/cm^3 ρS	Total porosity % ΦT	Open porosity to water % $ΦH_2O$	Open porosity to helium % ΦoHe	Closed porosity to helium % ΦcHe	Weight imbibition coefficient % ICw	Saturation index % SI	PLT strength index (MPa) $Is_{(50)}$
Fire ceramics	Un.samples	Average	1.85	2.62	2.70	32.3	26.1	29.2	3.1	14.1	89.5	2.98
		St. dev.	0.01	0.06	0.04	1.5	1.5	1.4	1.7	0.9	6.9	0.93
Food, liquid containers	Un.samples	Average	1.84	2.66	2.75	34.1	27.0	31.0	3.1	14.6	87.0	2.06
		St. dev.	0.03	0.06	0.08	2.1	1.2	1.7	1.6	0.7	4.6	0.58
Table ceramics	Un.samples	Average	1.86	2.64	2.74	33.5	27.7	29.5	4	14.9	93.9	2.4
		St. dev.	0.02	0.06	0.07	2	0.5	1.2	2.1	0.4	3.5	0.77
Fire ceramics	750 °C	Average	1.87	2.64	2.72	32.0	25.8	29.1	2.9	13.7	89.0	3.01
		St. dev.	0.05	0.07	0.07	2.8	1.1	2.0	2.4	0.7	5.6	0.90
Food, liquid containers	750 °C	Average	1.90	2.65	2.75	32.0	25.6	28.3	3.7	13.5	91.0	2.97
		St. dev.	0.05	0.07	0.05	1.3	1.2	1.5	1.1	0.7	7.5	0.68
Table ceramics	750 °C	Average	1.85	2.73	2.80	34.6	26.8	32.1	2.5	14.4	83.5	2.05
		St. dev.	0.02	0.04	0.06	2.1	1.2	1.4	1.2	0.8	2.8	1.05
Fire ceramics	1000 °C	Average	1.93	2.59	2.71	30.0	21.3	25.3	4.7	11.0	84.5	4.74
		St. dev.	0.02	0.05	0.08	2.7	1.5	1.3	2.4	0.9	8.1	3.31
Food, liquid containers	1000 °C	Average	1.97	2.62	2.75	30.0	21.6	24.8	5.2	10.9	87.0	3.37
		St. dev.	0.03	0.04	0.09	2.8	0.8	0.9	2.7	0.4	3.8	0.69
Table ceramics	1000 °C	Average	1.93	2.64	2.75	30.8	21.2	26.7	4.1	10.9	79.5	3.66
		St. dev.	0.04	0.03	0.04	1.6	0.7	1.4	1.7	0.6	3.2	1.41

34.1%, the highest values of closed helium porosity ($Φ_cHe$), 3.1%, and weight imbibition coefficient (IC_w), 14.6%; (ii) fire ceramics have the lowest values of total porosity ($Φ_T$), 32.3%, the highest values of strength index ($Is_{(50)}$), 2.98 MPa, and the lowest weight imbibition coefficient (ICw), 14.1%; (iii) food and liquid containers have the highest total porosity ($Φ_T$), 34.1%, open porosity ($Φ_OHe$), 31%, and the lowest mechanical strength ($Is_{(50)}$), 2.06 MPa.

Table ceramics are generally temporarily used to consume food, so no specific properties are required. In all table ceramics, Mr. Domingos used to prepare a clay mixture enriched in *strong* clay and in all cases a glaze cover is added to the objects surface. Just in one case (painted plate), it was not added. In order to understand the technological choice of Mr. Domingos (glaze application), we evaluated the effect of glaze on physical properties. The physical analyses (Fig. 10B) carried out on different sub-samples of table ceramics without and with glaze (also, in this case, we considered mean values for table ceramic with glaze and without glaze) show that the total porosity ($Φ_T$), the closed porosity to helium ($Φ_CHe$) and the open porosity to helium ($Φ_OHe$) are lower on sub-samples with glaze. Moreover, also weight imbibition coefficient (IC_w) is lower on the glazed sub-samples. If we consider thickness normalized water vapour permeability (Table 11), it is lower on sub-samples with glaze if compared with the only unglazed sub-samples. So, glaze application decreases the porosity and consequently the absorbed water. Thus, for the ceramist, it is not important the porosity, the ceramic paste can be more or less porous, because the surface of the object is sealed and impermeabilized by glaze application.

Fire ceramics are normally used to cook or to heat food (they are exposed to fire or to a heat source) and for this reason Mr. Domingos used a different clay mixture, more enriched in *weak* clay for their production. As a result, fire ceramics have the lowest total porosity ($Φ_T$), weight imbibition coefficient (ICw) and the highest PLT strength index if compared with food and liquid containers and table ceramics. If the specific function of these objects is considered (i.e. cooking food), the thermal conductivity must be as high as possible in order to transmit heat. As explained on different experimental test (Hein et al. 2008; Allegretta et al. 2014; Allegretta et al. 2017), total porosity ($Φ_T$) has a negative correlation with this property. Thus, fire ceramics must have low porosity in order to increase heat transfer (Roux 2019). If open porosity ($Φ_OHe$) and closed porosity ($Φ_CHe$) to helium are considered separately, they also behave differently to heat transfer. In particular, a certain degree of closed porosity favours heat transfer because it usually forms as a consequence of the densification of the ceramic paste, increasing thermal conductivity. In addition, ceramic with glazed (pot, *tacho*) and without glaze (pot lid,

Table 11 Permeability to water vapour results obtained for archaeological and traditional ceramic samples for different functional classes

Sample	Chronology, century	Typology	Function	Decoration	Permeability ($g/m^2 \times 24$ h)	Sample thickness (mm)	Permeability norm. ($g/m^2 \times 24$ h)/mm
[504]-4465	11th–12th	Pan	Fire ceramic	Unpainted	80.79	6.26	12.91
[504]-4660	11th–12th	Big jug	Food-liquid container	White painted	43.35	8.15	5.32
[504]-4464	11th–12th	Bowl	Table ceramic	White painted	115.36	7.8	14.79
[91]-1983	12th–13th	Lid	Fire ceramic	Unpainted	62.49	7.13	8.76
[2244]-15045	12th–13th	Pan	Fire ceramic	Unpainted	51.87	9.26	5.60
[91]-1978	12th–13th	Pot	Fire ceramic	Unpainted	48.63	4.73	10.28
[2244]-15029	12th–13th	Big jug	Food-liquid container	White painted	87.28	6.06	14.40
[91]-1985	12th–13th	Bowl	Table ceramic	Unpainted	61.85	5.56	11.12
[829]-6950	13th–14th	Lid	Fire ceramic	Unpainted	47.82	5.93	8.06
[829]-6953	13th–14th	Pan	Fire ceramic	Unpainted	51.02	6.63	7.70
[829]-6962	13th–14th	Bowl	Table ceramic	Unpainted	52.75	6.2	8.51
[2096]-14392	15th–16th	Pan	Fire ceramic	Unpainted	88.20	6.5	13.57
[2058]-14122	15th–16th	Bowl	Table ceramic	Unpainted	137.45	5.23	26.28
Pot lid	Modern	Pot lid	Fire ceramic	Unglazed	84.44	6.46	13.07
Pot	Modern	Pot	Fire ceramic	Glazed	90.42	6.43	14.06
Tacho	Modern	Tacho	Fire ceramic	Glazed	69.47	6.33	10.97
Chestnut roaster	Modern	Chestnut roaster	Fire ceramic	Unglazed	80.64	6.36	12.68
Jug	Modern	Jug	Food, liquid container	Unglazed	177.49	7.63	23.26
Water costrel	Modern	Water costrel	Food, liquid container	Unglazed	136.25	5.6	24.33
Jug lid	Modern	Jug lid	Food, liquid container	Unglazed	175.61	7.93	22.15
Yellow bowl	Modern	Yellow bowl	Table ceramic	Glazed	107.81	8.4	12.83
Bowl	Modern	Bowl	Table ceramic	Glazed	84.68	9	9.41
Green bowl	Modern	Green bowl	Table ceramic	Glazed	84.29	6.17	13.66
Glazed plate	Modern	Glazed plate	Table ceramic	Glazed	77.59	9.4	8.25
Painted plate	Modern	Painted plate	Table ceramic	Unglazed	167.41	6.73	24.88

chestnut roaster) have similar thickness normalized permeability (Table 11), much lower than table and food-liquid container ceramics, suggesting that glaze application does not influence significantly this property. This result indicates that the clay mix enriched in *weak* clay is definitely more suitable for the manufacture of fire ceramics and, in this particular case, vermiculite clay mineral favour the densification of the ceramic paste and the development of these specific characteristics (Sutcu 2015).

Food-liquid containers are normally used to store food and liquids and Mr. Domingos used a clay mixture, more enriched in *strong* clay for their production. As a consequence, like on table ceramics, food-liquid containers have the highest total (Φ_T) and open porosity (Φ_OHe) and the lowest mechanical strength ($Is_{(50)}$). Permeability is also very high for this functional class (Table 11). This reflects the production of the so-called hydro-ceramics, which are prepared in order to favour high porosity (in particular open porosity) and permeability. In fact, the ceramic paste must allow a thermal exchange (favoured by open porosity) by phase changing in order to ensure continuous condensation in the outer surface of ceramic artefact (Roux 2019). It is important to note that food-liquid containers were not covered by glaze.

Due to different porosities, and consequently also to the apparent density, the PLT strength index shows the different behaviour of the three functional subgroups, showing higher values on fire ceramics. A different trend of fire ceramics was also observed in lower real density and solid density values if compared with other functional subgroups.

The firing tests (Table 10, Fig. 10A) carried out on different sub-samples of traditional ceramics (at 750 and 1000 °C) showed that physical and mechanical characteristics changed.

Table 12 Medium values with standard deviation of physical and mechanical properties of archaeological ceramic samples (from different functional classes and chronology). When standard deviation is not reported, it means that just one sample was analysed

Century	Function		Apparent density g/cm^3 ρ_B	Real density g/cm^3 ρ_R	Solid density g/cm^3 ρ_S	Total Porosity % Φ_T	Open porosity to water % ΦoH_2O	Open porosity to helium % ΦoHe	Closed porosity to helium % ΦcHe	Weight imbibition coefficient % ICw	Saturation index % S.I.	PLT strength index (MPa) $Is_{(50)}$
11th–12th	Fire ceramics	Average	1.94	2.56	2.62	26.7	21.9	24.2	2.5	11.3	90.8	2.14
		St.dev.	0.04	0.00	0.02	0.8	0.4	1.6	0.8	0.4	4.9	0.66
	Food, liquid containers	Average	1.95	2.62	2.70	28.6	21.6	25.7	2.8	11.2	83.6	2.35
		St.dev.	0.07	0.02	0.07	0.2	3.7	1.9	1.7	2.3	9.0	0.83
	Table ceramics	Average	1.89	2.67	2.79	33.5	26.0	29.3	4.2	13.9	89.0	3.13
		St.dev.	0.01	0.01	0.02	1.0	0.4	0.0	1.1	0.3	1.2	0.39
12th–13th	Fire ceramics	Average	1.92	2.64	2.68	29.0	23.9	27.3	1.7	12.5	87.6	4.77
		St.dev.	0.03	0.03	0.05	2.3	2.2	1.3	1.0	1.4	5.2	1.79
	Food, liquid containers	Average	1.93	2.59	2.71	30.2	23.3	25.4	4.8	12.3	92.2	3.23
		St.dev.	0.03	0.04	0.05	3.3	0.9	2.1	2.3	0.8	5.5	0.51
	Table ceramics	Average	1.85	2.63	2.77	35.2	26.3	29.6	5.6	14.2	88.8	4.50
		St.dev.										
13th–14th	Fire ceramics	Average	1.95	2.61	2.72	29.4	21.8	25.4	4.0	11.2	86.4	4.07
		St.dev.	0.01	0.07	0.03	0.4	0.8	1.9	1.9	0.4	3.6	0.96
	Food, liquid containers	Average	1.87	2.73	2.77	32.8	28.7	31.5	1.3	15.3	91.2	4.17
		St.dev.										
	Table ceramics	Average	1.88	2.50	2.70	32.5	20.5	24.4	8.1	11.0	85.5	2.54
		St.dev.	0.04	0.10	0.06	2.8	2.1	4.6	1.8	1.2	7.7	1.29
15th–16th	Fire ceramics	Average	1.95	2.64	2.70	28.3	23.9	26.3	2.0	13.3	91.2	3.31
		St.dev.	0.07	0.01	0.02	3.0	2.1	2.8	0.9	0.4	6.2	0.67
	Food, liquid containers	Average	1.91	2.68	2.68	28.8	26.3	28.8	0.0	13.8	91.6	1.08
		St.dev.										
	Table ceramics	Average	1.90	2.62	2.70	30.2	24.2	27.3	2.9	12.8	88.2	2.63
		St.dev.	0.01	0.07	0.04	1.3	4.0	2.5	1.2	2.0	6.5	0.16

Table 13 Physical and mechanical properties of archaeological food and liquid containers from all periods

Century	Function	Samples	Typology	Apparent density	Real density	Solid density	Total porosity	Open porosity to water	Open porosity to helium	Closed porosity to helium	Weight imbibition coefficient	Saturation index	PLT strength index
				g/cm^3	g/cm^3	g/cm^3	%	%	%	%	%	%	(MPa)
				ρ_B	ρ_R	ρ_S	Φ_T	Φo H_2O	ΦoHe	ΦcHE	ICw	S.I.	$Is_{(50)}$
11th–12th	Food, liquid containers	[504]-4660	Big jug	2.00	2.64	2.75	28.5	17.3	24.3	4.2	8.7	71.3	2.13
		[504]-4666	Jug	1.99	2.64	2.74	28.3	21.2	24.4	3.9	10.6	86.8	3.46
		[475]-4467	Big earthen pot	1.85	2.59	2.60	28.8	26.3	28.4	0.4	14.2	92.6	1.48
12th–13th	Food, liquid containers	[2244]-15029	Big jug	1.98	2.57	2.63	25.5	22.1	22.9	2.6	11.1	96.4	3.67
		[91]-1981	Jug	1.91	2.55	2.76	33.2	24.2	25.3	7.9	13.2	95.6	2.51
		[91]-1979	Big earthen pot	1.90	2.64	2.74	31.8	23.6	28.0	3.9	12.4	84.5	3.50
13th–14th	Food, liquid containers	[829]-6966	Jug	1.87	2.73	2.77	32.8	28.7	31.5	1.3	15.3	91.2	4.16
15th–16th	Food, liquid containers	[2096]-14374	Big earthen pot	1.91	2.68	2.68	28.8	26.3	28.8	0.0	13.8	91.6	1.07

In particular, total porosity (Φ_T), open porosity to helium (Φ_OHe), open porosity to water ($\Phi_O H_2O$), saturation index (SI) and weight imbibition coefficient (IC_w) (Fig. 10C) decrease, while closed porosity to helium (Φ_CHe) and PLT strength index ($Is_{(50)}$) increase.

From the results of the firing tests, we can take an important general consideration. In ceramics with similar mineralogical and chemical composition, when the firing temperature of the ceramic product increases (see results in Tables 9 and 10), the original matrix porosity constantly decreases. This leads to a direct and constant negative correlation between the total porosity, Φ_T, and the firing temperature. Thus, the apparent density, ρB, inversely correlated to the total porosity, shows a clear positive correlation with the firing temperature of the ceramic product.

From these evidences, in the case of the untreated modern ceramics (Table 9), the total porosity (Φ_T) values of 33.3% indicate a firing temperature probably lower than 750 °C. A porosity reduction is observed starting from the first firing step at 750 °C (32.9%), with a further reduction at 1000 °C (30.3%).

Therefore, open porosity to helium (Φ_OHe) and water ($\Phi_O H_2O$), as well as the hydraulic properties (weight imbibition coefficients, IC_w, saturation index, SI), follow a negative correlation with the firing temperature (similar to the total porosity, Φ_T). This is generally followed by a positive correlation with the firing temperature of the closed porosity to helium, Φ_CHe, which after firing at 1000 °C reaches values between 4.1 and 5.2% (Table 10). This is the result of the progressive increase in shrinkage and compactness of the ceramic paste due to the thermal dehydroxylation of the clay minerals and the progressive vitrification of the ceramic paste, as evidenced by the identification of mullite on XRPD patterns.

Archaeological ceramics

In the case of archaeological samples, the results obtained after XRPD and XRF analyses showed that ceramics are quite homogeneous in term of mineralogical and chemical composition. Conversely OM observations showed that, depending on the functional class, ceramics were manufactured in a different way. In particular (see optical microscopy section), table and food-liquid containers were mainly produced using fabric 1–sub-fabric 1A, while in the case of fire ceramics, fabric 1–sub-fabric 1B was utilized. These observations have been further supported by physical and mechanical properties. Actually, they are quite heterogeneous but, considering mean values for different chronological period (Table 12), each functional class have specific characteristics, similar to that observed for traditional ceramics such as (i) table ceramics from each period have highest total (Φ_T), 30.2–35.2%, and closed porosities (Φ_CHe), 2.9–8.1%; (ii) fire ceramics have the lowest total porosity (Φ_T), 26.7–29.4%, in every chronological period; (iii) food and liquid container gave heterogeneous results, which will be explained in detail.

This suggests that ancient ceramists used a specific ceramic paste to obtain specific technological characteristics along time. In any case, it is not possible to understand whether different raw materials (i.e. temper and/or clay) were mixed.

Regarding table ceramics, the high total (Φ_T) and closed porosity to helium (Φ_CHe) is the result of a specific technological choice. Considering that firing temperature and total porosity are inversely correlated (Kam et al. 2009; De Bonis et al. 2014; Cultrone et al. 2004), the identification of illite/muscovite, but not mullite (Table 4), suggests low degree of vitrification of the ceramic paste. At the same time firing temperature and closed porosity to helium (Φ_CHe) are linearly correlated. This correlation was also evident during the firing test carried out on traditional ceramics. In the case of archaeological table ceramics, it was the result of a slip application, as highlighted during OM observations. Slip is usually applied to increase waterproof characteristics of the outer ceramic surface (Roux 2019) before firing. This hypothesis was tested by permeability tests (Table 11). Results for table ceramics, especially thickness normalized permeability values, apparently show heterogeneous results. This can be the consequence of several factors such as ceramist expertise, shaping technique, surface treatments (slip, glaze layer) and chemical-physical alteration degree of the artefact surface. Consequently, in some cases permeability is low (8.51, 11.12 $g/m^2 \times 24$ h/mm), similar to those observed on modern traditional ceramics covered by glaze (8.25, 9.41 $g/m^2 \times 24$ h/mm). Just in one case (sample [2058]-14122 from the fifteenth–sixteenth century) permeability was very high (26.28 41 $g/m^2 \times 24$ h/mm) suggesting, in this case, surface alteration and/or a bad surface treatment. From these observations, also archaeological table ceramics could be more or less porous and surface treatments (i.e. slip application) were supposed to impermeabilize the object surface.

Fire ceramics have the lowest total porosity (Φ_T). Also, permeability is low, similar and even smaller to that obtained for traditional ceramics. These results are significant to understand the manufacturing technologies, indicating that similar criteria were adopted for the production of fire ceramics both in ancient time and in modern traditional ceramics.

Regarding archaeological food and liquid containers (Table 13), they have a slightly different function, namely to store liquid (jug, big jug) and food (big earthen pot). Usually total porosity (Φ_T), open porosity to helium (Φ_OHe) and open porosity to water ($\Phi_O H_2O$) are higher on big earthen pots, while closed porosity to helium (Φ_CHe) is higher on jug and big jugs (Fig. 10D). The only exception is the jug [829]-6966 from the thirteenth–fourteenth century (Table 13), which is similar to big earthen pots. This difference is also shown by OM, especially in the amount of temper, grain size and porosity, higher on big earthen pots. Regarding permeability it was

possible to perform analyses just on two samples of big jugs from the eleventh–twelfth and twelfth–thirteenth century (samples [504]-4660, [2244]-15029). Normalized permeability results (Table 11) shows medium-low values, especially if compared with modern traditional ceramics with the same function (jug and water costrel). So, if we consider that a good liquid container needs high total porosity (Φ_T), open porosity to helium ($\Phi_O He$) and water ($\Phi_O H_2O$) in order to favour liquid coolness (Roux 2019), archaeological ceramics were less efficient than traditional ones. In the case of big earthen pots and jug [829]-6966, porosity was probably important, because it could act as insulating barrier against the external environment.

In the case of PLT strength index ($Is_{(50)}$), it was not possible to establish a correlation with the firing temperature, as established for modern traditional ceramics, due to sampling restriction. Generally, in the case of archaeological ceramics of all periods, $Is_{(50)}$ decrease when the amount of temper increases and when temper grain size is bigger. Similar results were obtained and discussed by De Bonis et al. (2014) and Müller et al. (2010).

By a comparison of mean physical data (Table 9) between archaeological and traditional ceramics, some general considerations can be made, especially about the relationship between firing temperature and physical properties on archaeological ceramics. As explained above, total porosity (Φ_T) varies according to the firing temperature (Kam et al. 2009) and, a significant porosity decrease usually happens above 900–950 °C accompanied by the complete dehydroxylation of clay minerals and the formation of high temperature mineralogical phases (De Bonis et al. 2014; Cultrone et al. 2004). These results were also highlighted by the experimental firing test carried out on traditional ceramics sub-samples. Considering that archaeological ceramics have values of total porosity, (Φ_T), between 29 and 31% vol., therefore similar to the modern ceramics fired at 1000 °C (which have values of the same property around 30%), it is probable that the firing temperature of archaeological ceramics varies between 800 and 1000 °C. Those belonging to the eleventh–twelfth and fifteenth–sixteenth century were probably fired around 950 °C, while those of the twelfth–thirteenth and thirteenth–fourteenth century were fired at lower temperature, probably around 800–850 °C. These observations are in agreement with XRPD data.

Conclusion

In this work, two different groups of artefacts, archaeological and traditional ceramics, with different functions and chronology, have been analysed. Our results showed that the methodology applied was effective to compare pottery technology between the Middle Ages and Modern times. Moreover, it was also possible to extract some important methodological considerations. Both ceramic groups were produced with local raw materials, extracted in different area, in Santarém and Muge, respectively, but geologically similar. Physical and mechanical tests were essential in order to establish the characteristics of different functional objects. In fact, archaeological and traditional ceramics were produced following specific technological criteria, mainly linked to the final object function and ceramic behaviour. However, this goal was achieved by two different approaches, which differs in the preparation of the ceramic paste and on the firing temperature:

- For archaeological samples, the ceramic paste was prepared differently for different functions of the objects. Actually, as evidenced by OM, kitchen and food/liquid container ceramics are different from fire ceramics. These differences mainly reside on temper characteristics and they were not evident neither after XRD nor chemical analyses. Only MO shows significant differences. At this stage, it is not possible to assess if distinct clays were mixed. The ceramic production is specialized along time;
- In the case of traditional samples, the ceramic paste was prepared similarly in every case, with similar amount and temper characteristics, changing the proportion of *strong* and *weak* clay. Nevertheless, the effect of mixing different raw materials (clay) is not identifiable neither by OM, chemical and XRD analyses;
- Regarding firing temperature, archaeological ceramics were fired at higher temperature if compared with traditional ones. This was evidenced by the linear correlation between firing temperature and total porosity established by different firing test on traditional ceramics.

Considering OM, XRPD and XRF results, archaeological ceramics raw material sources, in particular clay and temper, were widely available in every chronological period indicating ceramic production continuity using the sedimentary deposits close of the city of Santarém. Consequently, we suppose that fuel and water were also easily available for ceramic production in the Middle Ages. Regarding ceramic with the same function, results did not detect any significant difference in pottery characteristics. Also, historical sources and archaeological data attest pottery production continuity in the town along time. These observations suggest that the ceramic cycle and technology of production were not affected by political and economic modification, occurred between the eleventh and sixteenth century. In particular as discussed along the manuscript, ceramic production during the Middle Ages was quite specialized suggesting, another time, expertise continuity. We can also sustain that, in the case of both Middle Ages ceramics from Santarém and the traditional ceramics from Muge, the ceramic characteristics and technology were mainly determined by

local socio-cultural factors. Basing on this research, we do not have data to state that religion, ideology and ethnicity have never played a role in the productive ceramic cycle. Actually, the archaeological record of the city evidenced a conservation of the Islamic characters during the Middle Ages. As evidenced by historical sources Christians, Muslim and Jewish lived together in the same town in the timeframe considered. Actually, during history, to a modification of the ruling power do not usually corresponded a radical substitution of the local population. So, the technical expertise is more probably the result of a local tradition started, in the case of this specific manuscript, during the Islamic period. In any case, our data show that every decision or technical choice was taken depending on the functional and performance characteristics desired for a specific artefact. In this case, ceramists' technical expertise was the main factor that could really influence pottery technology in the creation of a specific object. So, since the Middle Ages, ceramics were produced following specific criteria and ancient technical expertise is still valid nowadays.

Acknowledgements The first author wants to acknowledge the Unesco Chair in Intangible Heritage and Traditional Know-How: Linking Heritage of the University of Évora for the PhD scholarship. The first author wishes also to acknowledge Mr. Domingos for his precious help and availability for the development of this work and the precious suggestions of the referees.

Funding information This work was funded by FEDER founds in the framework of the new agreement PT2020 and by Nationals Founds of the FCT/MEC – Science and Technology Foundation of the Projects UID/Multi/04449/2013 (POCI-01-0145-FEDER-007649) (Laboratório HERCULES/UÉ) and UID/HIS/00057 – POCI-01-0145-FEDER-007702 (CIDEHUS/UÉ). Moreover, this work was supported by an agreement between the University of Évora and the University of Cagliari to Cultural Heritage research.

References

Adams EA, Mackenzie WS, Guilford C (1984) Atlas of sedimentary rock under the microscopes. Longman Sc. longman Group, Harlow

Allegretta I, Eramo G, Pinto D, Hein A (2014) The effect of temper on the thermal conductivity of traditional ceramics: nature, percentage and granulometry. Thermochim Acta 581. https://doi.org/10.1016/j.tca.2014.02.024

Allegretta I, Eramo G, Pinto D, Hein A (2017) The effect of mineralogy, microstructure and firing temperature on the effective thermal conductivity of traditional hot processing ceramics. Appl Clay Sci 135: 260–270. https://doi.org/10.1016/j.clay.2016.10.001

Alves Conde MS (2005) Fronteira, guerra e organização social do espaço: o Vale do Tejo entre muçulmanos e cristão. In: Barroca MJ, Ferreira Fernandes IC (eds) Muçulmanos e Cristão entre o Tejo e o Douro (Sécs. VIII a XIII). Câmara Municipal de Palmela - Faculdade de Letras Universidade do Porto, Palmela, pp 43–52

Arnold DE (2000) Does the standardization of ceramic really mean specialization? J Archaeol Method Theory 7:333–375. https://doi.org/10.1023/A:1026570906712

Arruda AM (1993) A ocupação da Idade do Ferro da Alcaçova de Santarém no contexto da expansão Fenícia na fachada Atlântica peninsular. Estud Orientais 4:193–214

Arruda AM, Viegas C (1999) Cerâmicas islâmicas da Alcáçova de Santarém. Rev Port Arqueol 2:105–186

Arruda AM, Pereira C, Pimenta J et al (2016) As contas de vidro do Porto do Sabugeiro (Muge, Salvaterra de Magos, Portugal) / Glass beads from Porto do Sabugeiro (Muge, Salvaterra dos Magos, Portugal). Cuad Prehist y Arqueol 42:79–101. https://doi.org/10.15366/cupauam2016.42.002

Barroca MJ (2003) Da Reconquista a D. Dinis. In: Mattoso J (ed) Nova História Militar de Portugal, vol I. Circulo de Leitores, Lisboa, pp 20–161

Barros MFL (2004) Os mouros de Santarém. A comuna e os espaço. In: Amado C, Mata L (eds) Santarém e o Magreb: encontro secular (970–1578). Museo municipal de Santarém - Câmara Municipal de Santarém, Santarém

Beltrame M, Liberato M, Mirão J et al (2019) Islamic and post Islamic ceramics from the town of Santarém (Portugal): the continuity of ceramic technology in a transforming society. J Archaeol Sci Reports 23:910–928. https://doi.org/10.1016/j.jasrep.2018.11.029

Bugalhão J, Folgado D (2001) O arrabalde ocidental da Lisboa islâmica: urbanismo e produção oleira. Arqueol Mediev 7:111–145

Buxeda I, Garrigós J, Cau Ontiveros MA, Kilikoglou V (2003) Chemical variability in clays and pottery from a traditional cooking pot production village: testing assumptions in Pereruela. Archaeometry 45: 1–17. https://doi.org/10.1111/1475-4754.00093

Cantin N, Mayor A (2018) Ethno-archaeometry in eastern Senegal: the connections between raw materials and finished ceramic products. J Archaeol Sci Reports 21:1181–1190. https://doi.org/10.1016/j.jasrep.2017.01.015

Casimiro TM, Boavida C, Silva T (2018) Ceramics and cultural change in medieval (14th-15th century) Portugal. The case of post-Reconquista Santarém. Mediev Ceram 37:21–36

Catarino H (1995) A occupação Islamica. In: Medina J (ed) História de Portugal: Dos tempos Pré-Histórico aos nossos dias. Vol 3: O Mundo Luso-Romano. Amadora Clube Internacional do Livro, Madrid, pp 267–349

Cau Ontiveros MA, Montana G, Tsantini E, Randazzo L (2015) Ceramic ethnoarchaeometry in Western Sardinia: production of cooking ware at Pabillonis. Archaeometry 57:453–475. https://doi.org/10.1111/arcm.12100

Coll Conesa J, Porras García A (2010) Tipología, cronología y producción de los hornos cerámicos en al-Andalus. In: Arqueol. Mediev. http://www.arqueologiamedieval.com/articulos/125/tipologia-cronologia-y-produccion-de-los-hornos-ceramicos-en-al-andalus. Accessed 30 Apr 2019

Columbu S, Antonelli F, Lezzerini M et al (2014a) Provenance of marbles used in the Heliocaminus baths of Hadrian's Villa (Tivoli, Italy). J Archaeol Sci 49:332–342. https://doi.org/10.1016/j.jas.2014.05.026

Columbu S, Gioncada A, Lezzerini M, Marchi M (2014b) Hydric dilatation of ignimbritic stones used in the church of Santa Maria di Otti (Oschiri, northern Sardinia, Italy). Ital J Geosci 133:149–160. https://doi.org/10.3301/IJG.2013.20

Columbu S, Cruciani G, Fancello D et al (2015a) Petrophysical properties of a granite-protomylonite-ultramylonite sequence: insight from the Monte Grighini shear zone, central Sardinia, Italy. Eur J Mineral 27: 471–486. https://doi.org/10.1127/ejm/2015/0027-2447

Columbu S, Sitzia F, Verdiani G (2015b) Contribution of petrophysical analysis and 3D digital survey in the archaeometric investigations of

the Emperor Hadrian's Baths (Tivoli, Italy). Rend Lincei 26:455–474. https://doi.org/10.1007/s12210-015-0469-3
Columbu S, Lisci C, Sitzia F, Buccellato G (2017a) Physical–mechanical consolidation and protection of Miocenic limestone used on Mediterranean historical monuments: the case study of Pietra Cantone (southern Sardinia, Italy). Environ Earth Sci 76. https://doi.org/10.1007/s12665-017-6455-6
Columbu S, Sitzia F, Ennas G (2017b) The ancient pozzolanic mortars and concretes of Heliocaminus baths in Hadrian's Villa (Tivoli, Italy). Archaeological and Anthropological Sciences
Conshohocken W (2005) ASTM D5731-95: standard test method for determination of the point load strength index of rock 1. Rock Mech 22:1–7
Cultrone G, Rodriguez-Navarro C, Sebastian E et al (2001) Carbonate and silicate phase reactions during ceramic firing. Eur J Mineral 13:621–634. https://doi.org/10.1127/0935-1221/2001/0013-0621
Cultrone G, Sebastián E, Elert K et al (2004) Influence of mineralogy and firing temperature on the porosity of bricks. J Eur Ceram Soc 24:547–564. https://doi.org/10.1016/S0955-2219(03)00249-8
Cunha PP (2019) Cenozoic basins of Western Iberia: Mondego, lower Tejo and Alvalade basins. In. Quesada C., Oliveira J.T. (eds) The Geology of Iberia: A Geodynamic Approach, Volume 4 – Cenozoic Basins, Springer International Publishing, pp 105–130
Cunha PP, Martins AA, Daveau S, Friend PF (2005) Tectonic control of the Tejo river fluvial incision during the late Cenozoic, in Ródão - Central Portugal (Atlantic Iberian border). Geomorphology 64:271–298. https://doi.org/10.1016/j.geomorph.2004.07.004
D'Ercole G, Garcea EAA, Eramo G, Muntoni IM (2017) Variability and continuity of ceramic manufacturing of prehistoric pottery from upper Nubia, Sudan: an ethnographic comparison. J Archaeol Sci Reports 16:553–563. https://doi.org/10.1016/j.jasrep.2017.04.012
De Bonis A, Cultrone G, Grifa C et al (2014) Clays from the Bay of Naples (Italy): new insight on ancient and traditional ceramics. J Eur Ceram Soc 34:3229–3244. https://doi.org/10.1016/j.jeurceramsoc.2014.04.014
Dondi M, Principi P, Raimondo M, Zanarini G (2003) Water vapour permeability of clay bricks. Constr Build Mater 17:253–258. https://doi.org/10.1016/S0950-0618(02)00117-4
Douglass LA (1989) Vermiculites. In: Dixon JB, Weed SB (eds) Minerals in soil environments, 2nd edn. Soil Scien. Soil Science Society of America, Madison, pp 625–674
El Ouahabi M, Daoudi L, Hatert F, Fagel N (2015) Modified mineral phases during clay ceramic firing. Clay Clay Miner 63:404–413. https://doi.org/10.1346/CCMN.2015.0630506
Fabbri B, Gualtieri S, Shoval S (2014) The presence of calcite in archeological ceramics. J Eur Ceram Soc 34:1899–1911. https://doi.org/10.1016/j.jeurceramsoc.2014.01.007
Fernandes IC, Martínez SG, Gonçalves MJ et al (2016) O comércio da Corda Seca (Total e Parcial) no Gharb al-Ândalus. Actas do X Congresso de Cerâmica Medieval no Mediterrâneo. In: Martínez SG, Gonçalves MJ (eds) Actas do X Congresso Iinternacional "A Cerâmica Medieval no Mediterrâneo", Silves-Mértola, 22 a 27 de Outubro de, vol 2012. Campo Arqueológico de Mértola, Câmara Municipal de Silves, Loule, pp 649–666
Folk RL (1959) American Association of Petroleum Geologists Practical petrographic classification of limestones. Bull Am Assoc Pet Geol 43. https://doi.org/10.1306/0BDA5C36-16BD-11D7-8645000102C1865D
García Fitz F (2009) La Reconquista: un estado de la cuestión. Clío Crímen Rev del Cent Hist del Crim Durango 6:142–215
Garcia y Garcia A (2007) La conquista de Santarém en el contexto de la cruzada Ibérica. In: Nelson Ferrão H (ed) Santarém na Idade Média: Actas do colóquio 13–14 Março 1998. Câmara Municipal de Santarém, Santarém, pp 101–106
Georgiou CD, Sun HJ, McKay CP, Grintzalis K, Papapostolou I, Zisimopoulos D, Panagiotidis K, Zhang G, Koutsopoulou E, Christidis GE, Margiolaki I (2015) Evidence for photochemical production of reactive oxygen species in desert soils. Nat Commun 6:7100. https://doi.org/10.1038/ncomms8100
Gomes Pinto CG (2012) Gestos, memórias e formas materiais legadas pelo barro. A produção olárica no Ribatejo na coleção de olaria traditional do Museu nacional de Etnologia. Universidade Nova de Lisboa
Gosselain OP (1992) Bonfire of the enquiries. Pottery firing temperatures in archaeology: what for? J Archaeol Sci 19:243–259. https://doi.org/10.1016/0305-4403(92)90014-T
Gosselain OP (2012) Technology, Oxford Han. Oxford University Press, Oxford
Goudarzi MA, Landry RJ (2017) Assessing horizontal positional accuracy of Google Earth imagery in the city of Montreal, Canada. Geod Cartogr 43:56–65. https://doi.org/10.3846/20296991.2017.1330767
Heimann RB, Maggetti M (2014) Ancient and historical ceramics. Materials, technology, art and culinary tradition. Schweizerbart Science Pubblisher, Stuttgrat
Heimann RB, Maggetti M (2016) The struggle between thermodynamics and kinetiks: phase evolution of ancient and historical ceramics. In: Oberti R (ed) Artioli G. Emu Notes in Mineralogy, Recent Con
Hein A, Müller NS, Day PM, Kilikoglou V (2008) Thermal conductivity of archaeological ceramics: the effect of inclusions, porosity and firing temperature. Thermochim Acta 480:35–42. https://doi.org/10.1016/j.tca.2008.09.012
Hubbard CR, Evans EH, Smith DK (1976) The reference intensity ratio, I / I c , for computer simulated powder patterns. J Appl Crystallogr 9:169–174. https://doi.org/10.1107/S0021889876010807
Jordán MM, Boix A, Sanfeliu T, De La Fuente C (1999) Firing transformations of cretaceous clays used in the manufacturing of ceramic tiles. Appl Clay Sci 14:225–234. https://doi.org/10.1016/S0169-1317(98)00052-0
Kam S, Zerbo L, Bathiebo J et al (2009) Permeability to water of sintered clay ceramics. Appl Clay Sci 46:351–357. https://doi.org/10.1016/j.clay.2009.09.005
Kilikoglou V, Vekinis G, Maniatis Y, Day PM (1998) Mechanical performance of quartz-tempered ceramics: part I, strength and toughness. Archaeometry 40:261–279. https://doi.org/10.1111/j.1475-4754.1998.tb00837.x
Kresten P, Berggren G (1978) The thermal decomposition of vermiculite. Thermochim Acta 23:171–182. https://doi.org/10.1016/0040-6031(78)85123-5
Lehroi-Gourhan A (1964) Le geste et la Perole. Tome I Technique et linguage. A. Michel, Paris
Lemonier P (1993) Technological choises: transformation in material culture since the neolithic. Routledge, London
Lepierre C (1899) Estudo chimico e technologico sobre a ceramica portugueza moderna. Imprensa Nacional, Lisboa
Liberato M (2012) Cerâmica pintada a branco na Santarém Medieval, Uma abordagem diacrónica: séculos XI a XVI. Master Thesis in Archaeology University of Lisbon
Liberato M (2016) Cerâmica Pintada a Branco na Santarém Medieval. Séculos XI-XVI. In: Martínez SG, Gonçalves MJ (eds) Actas do X Congresso Iinternacional "A Cerâmica Medieval no Mediterrâneo". Silves-Mértola, 22 a 27 de Outubro de 2012. Campo Arqueológico de Mértola, Câmara Municipal de Silves, Loule, pp 777–791
Lindahl A, Pikirayi I (2010) Ceramics and change: an overview of pottery production techniques in northern South Africa and eastern Zimbabwe during the first and second millennium AD. Archaeol Anthropol Sci 2:133–149. https://doi.org/10.1007/s12520-010-0031-2
Livingstone Smith A (2000) Processing clay for pottery in northern Cameroon: social and technical requirements. Archaeometry 42:21–42. https://doi.org/10.1111/j.1475-4754.2000.tb00864.x
Lopes G (2015) Materiais do povoado Islâmico do Serradinho (Muge, Salvaterra de Magos). Cira Arqueol 4:171–186

Maggetti M, Galletti G (1982) Die Referenzgruppe(n) Lousanna - mineralogische und chemische Untersuchungen der keramischen Produktion der Topferwerkstatten Berna. Schweizerischen Gesellschaft fur Ur- und Furhgeschichte:109–132

Maniatis Y, Tite MS (1981) Technological examination of Neolithic-Bronze Age pottery from central and southeast Europe and from the Near East. J Archaeol Sci 8:59–76. https://doi.org/10.1016/0305-4403(81)90012-1

Maniatis Y, Simopoulos A, Kostikas A (1981) Moessbauer study of the effect of calcium content on iron oxide transformations in fired clays. J Am Ceram Soc 64:263–269. https://doi.org/10.1111/j.1151-2916.1981.tb09599.x

Maritan L, Nodari L, Mazzoli C et al (2006) Influence of firing conditions on ceramic products: experimental study on clay rich in organic matter. Appl Clay Sci 31:1–15. https://doi.org/10.1016/j.clay.2005.08.007

McConville CJ, Lee WE (2005) Microstructural development on firing illite and smectite clays compared with that in kaolinite. J Am Ceram Soc 88:2267–2276. https://doi.org/10.1111/j.1551-2916.2005.00390.x

Moore DM, Reynolds RC (1997) X-ray diffraction and the identification and analysis of clay minerals. Oxford University Press, Oxford

Müller NS, Kilikoglou V, Day PM, Vekinis G (2010) The influence of temper shape on the mechanical properties of archaeological ceramics. J Eur Ceram Soc 30:2457–2465. https://doi.org/10.1016/j.jeurceramsoc.2010.04.039

Nodari L, Marcuz E, Maritan L et al (2007) Hematite nucleation and growth in the firing of carbonate-rich clay for pottery production. J Eur Ceram Soc 27:4665–4673. https://doi.org/10.1016/j.jeurceramsoc.2007.03.031

Noll W, Heimann RB (2016) Ancient Old World pottery. Materials, technology, and decoration. E. Schweizerbart'Sche Varlagsbuchhandlung Pubblisher, Stuttgrat

Normal (1985) Istitiuto Centrale del Restauro - Commissione Normal (I.C.R.-C.N.R), 1985. Alterazioni dei materiali lapidei e trattamenti conservativi. Proposte per l'unificazione dei metodi sperimentali di studio e di controllo. Permeabilità al vapor d'acqua. Doc. Normal 21/85

Pais J (2004) The Neogene of the Lower Tagus Basin (Portugal). Rev Española Paleontol 19:229–242

Pulighe G, Baiocchi V, Lupia F (2016) Horizontal accuracy assessment of very high resolution Google Earth images in the city of Rome, Italy. Int J Digit Earth 9:342–362. https://doi.org/10.1080/17538947.2015.1031716

Quinn PS (2013) Ceramic petrography. The interpretation of archaeological pottery & related artefacts in thin section. Archaeopress, Oxford

Riccardi MP, Messiga B, Duminuco P (1999) An approach to the dynamics of clay firing. Appl Clay Sci 15:393–409. https://doi.org/10.1016/S0169-1317(99)00032-0

Rodriguez-Navarro C, Cultrone G, Sanchez-Navas A, Sebastian E (2003) TEM study of mullite growth after muscovite breakdown. Am Mineral 88:713–724. https://doi.org/10.2138/am-2003-5-601

Rodriguez-Navarro C, Ruiz-Agudo E, Luque A et al (2009) Thermal decomposition of calcite: mechanisms of formation and textural evolution of CaO nanocrystals. Am Mineral 94:578–593. https://doi.org/10.2138/am.2009.3021

Romão J, Metodiev D, Dias R, Ribeiro A (2013) Evolução geodiâmica dos sectores meridionais da Zona Centro-Ibérica. In: Dias R, Araújo A, Terrinha P, Kullberg JC (eds) Geologia de Portugal, vol. I. Geologia Pré-mesozóica de Portugal. Escolar Editora, Lisboa, pp 205–258

Roux V (2019) Ceramics and society: a technological approach to archaeological assemblages. Springer Nature Switzerland

Santos Júnior J (1932) Olarias de muge: Notas Etnográficas. Trabalhos de Antropologia e Etnologia 5:217–226

Schiffer MB, Skibo JM (1987) Theory and experiment in the study of technological change. Curr Anthropol 28:595–622. https://doi.org/10.1086/203601

Schiffer MB, Skibo JM (1997) The explanation of artifact variability. Am Antiq 62:27–50. https://doi.org/10.2307/282378

Sidarus AY (2007) Shantarîn/Santarém, fronteira ambivalente Islamo-Cristã. In: Nelson Ferrão H (ed) Santarém na Idade Média: Actas do colóquio 13-14 Março 1998. Camara Municipale de Santarém, Santarém, pp 319–336

Sillar B (2000) Dung by preference: the choice of fuel as an example of how Andean pottery production is embedded within wider technical, social, and economic practices. Archaeometry 42:43–60. https://doi.org/10.1111/j.1475-4754.2000.tb00865.x

Silva J, de Brito J, Veiga R (2009) Incorporation of fine ceramics in mortars. Constr Build Mater 23:556–564. https://doi.org/10.1016/j.conbuildmat.2007.10.014

Sutcu M (2015) Influence of expanded vermiculite on physical properties and thermal conductivity of clay bricks. Ceram Int 41:2819–2827. https://doi.org/10.1016/j.ceramint.2014.10.102

Tite MS, Sillar B (2000) The challenge of "technological choices" for materials science approaches in archaeology. Archaeometry 42:2–20

Trindade MJ, Dias MI, Coroado J, Rocha F (2009) Mineralogical transformations of calcareous rich clays with firing: a comparative study between calcite and dolomite rich clays from Algarve, Portugal. Appl Clay Sci 42:345–355. https://doi.org/10.1016/j.clay.2008.02.008

V. da Rocha Beirante MA (1980) Santarém Medieval. Universidade Nova de Lisboa, Faculdade de Ciências Sociais e Humanas, Lisboa

Wang Y, Zou Y, Henrickson K et al (2017) Google Earth elevation data extraction and accuracy assessment for transportation applications. PLoS One 12:1–17. https://doi.org/10.1371/journal.pone.0175756

Zbyszewsky G (1953) Geological map of Portugal, scale 1:50000, with esplicative notes. Map 31-A, Santarém

Zbyszewsky G, Da Viega Ferreira O (1968) Geological map of Portugal, scale 1:50000, with esplicative notes. Map 31-C, Coruche

Publisher's note Springer Nature remains neutral with regard to jurisdictional claims in published maps and institutional affiliations.